

AMERICAN UNIVERSITY OF BEIRUT

RECONFIGURABLE, MINIATURIZED, AND COGNITIVE
ANTENNAS FOR IOT DEVICES

by

ROSETTE MARIA MOUNIR BICHARA

A thesis
submitted in partial fulfillment of the requirements
for the degree of Master of Engineering
to the Department of Electrical and Computer Engineering
of the Maroun Semaan Faculty of Engineering and Architecture
at the American University of Beirut

Beirut, Lebanon
April 2019

AMERICAN UNIVERSITY OF BEIRUT

RECONFIGURABLE, MINIATURIZED, AND COGNITIVE
ANTENNAS FOR IOT DEVICES

by
ROSETTE MARIA MOUNIR BICHARA

Approved by:

Prof. Joseph Costantine, Associate Professor
Electrical and Computer Engineering



Advisor

Prof. Mariette Awad, Associate Professor
Electrical and Computer Engineering



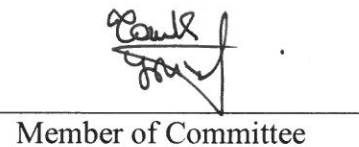
Co-Advisor

Prof. Rouwaida Kanj, Assistant Professor
Electrical and Computer Engineering



Member of Committee

Prof. Youssef Tawk, Assistant Professor
Electrical and Computer Engineering



Member of Committee

Date of thesis defense: April 24th, 2019

AMERICAN UNIVERSITY OF BEIRUT

THESIS, DISSERTATION, PROJECT RELEASE FORM

Student Name:

Hounis Bichana Rosette Maria
Middle Last First

Master's Thesis Master's Project Doctoral Dissertation

I authorize the American University of Beirut to: (a) reproduce hard or electronic copies of my thesis, dissertation, or project; (b) include such copies in the archives and digital repositories of the University; and (c) make freely available such copies to third parties for research or educational purposes.

I authorize the American University of Beirut, to: (a) reproduce hard or electronic copies of it; (b) include such copies in the archives and digital repositories of the University; and (c) make freely available such copies to third parties for research or educational purposes after:

One ---- year from the date of submission of my thesis, dissertation, or project.

Two ---- years from the date of submission of my thesis, dissertation, or project.

Three ---- years from the date of submission of my thesis, dissertation, or project.

Rosette Maria

Signature

6/5/2019

Date

ACKNOWLEDGMENTS

A very special gratitude goes out to my advisors, Prof. Joseph Costantine and Prof. Mariette Awad who always helped and guided me through my years at AUB, they always steered me in the right the direction whenever they thought I needed it. It was enriching to have the opportunity to work with them.

I am grateful to my father Mounir, my mother Micheline and my siblings Louise, Elie and Carine who have provided me through moral and emotional support in my life. I am also grateful to my other family members who have supported me along the way.

And finally, last but by not least, I would like to thank my AUB friends who were like a second family to me and with whom I had a very beautiful time.

AN ABSTRACT OF THE THESIS OF

Rosette Maria Mounir Bichara for Master of Engineering
Major: Electrical and Computer Engineering

Title: Reconfigurable, miniaturized, and cognitive antennas for IOT devices

In recent years, the advancements in wireless communications imposed the need of an intelligent Wireless system conscious of its environment and capable of changing its operating frequency, modulation, waveform and transmitting power. Such advancements are accompanied by an imbalance use of the spectrum where some frequency bands are overloaded while others often remain idle. As a solution to the spectrum imbalance, cognitive radio enables sensing the spectrum, learning its activities and identifying the suitable frequencies for communication. Once such frequencies are identified, antennas are ordered to reconfigure their topology through software in order to achieve a successful communication across the desired bands.

Cognitive radio becomes a necessity in the era of Internet of things (IoT), as millions of devices must be connected and able to communicate on demand. Enabling such devices to communicate requires the integration of agile reconfigurable antennas within their communication systems. Hence, such antennas must be miniature in size, reconfigurable and easily software controlled. At the same time these antennas must be able to preserve acceptable radiation efficiencies, stable radiation patterns and constant gains.

In this thesis the challenge of proposing a new antenna design that is miniature in size and exhibit an acceptable radiation performance is tackled. Furthermore, machine learning techniques come at the core of such design requirements by providing optimization tools that allow the successful miniaturization of the antenna structure while satisfying all the required constraints. In fact, techniques such as genetic algorithm and quantum genetic algorithm can be employed to generate three dimensional and volumetric antenna structures that can be integrated in compact IoT devices within a Dynamic cognitive radio setting. This thesis also addresses the integration of switching components within the antenna topology in order to reconfigure its operation. Such integration benefits as well from artificial intelligence and machine learning techniques to estimate with great accuracy the predicted performance and optimal antenna integration. Finally the thesis concludes with a full implementation of IoT integrated, machine learning defined, reconfigurable antenna components that can be optimally integrated within the future millions of connected devices.

CONTENTS

ACKNOWLEDGEMENTS	v
ABSTRACT.....	vi
LIST OF ILLUSTRATIONS.....	x
LIST OF TABLES.....	vii

Chapter

I. INTRODUCTION.....	1
A. Background and motivation.....	1
B. Thesis structure.....	3
II. OVERVIEW OF ANTENNAS FOR IOT	4
A. Introduction	4
B. Electrical small antennas	4
C. Miniaturization techniques	5
1. Overview.....	5
2. Miniaturized antennas.....	9
D. Reconfiguration	10
1. Overview.....	10
2. Reconfigurable antennas.....	12
E. Conclusion.....	15
III. MACHINE LEARNING ALGORITHMS APPLIED ON ANTENNA STRUCTURES.....	16
A. Introduction.....	16

B. Genetic Algorithm.....	16
1. Overview.....	16
2. Antenna design using GA.....	17
C. Quantum Genetic Algorithm.....	23
1. Overview	23
2. Quantum gate	25
3. QGA applications.....	26
D. Conclusion.....	27
IV. NEW ANTENNA DESIGNS FOR IOT.....	28
A. Introduction.....	28
B. Automation part.....	28
C. MATLAB code for automation.....	29
1. GA automation code.....	29
2. QGA automation code	30
D. Fitness function.....	32
1. Simple fitness.....	33
2. Reconfigurable fitness	33
E. Antenna designs.....	34
1. Design one: Folded miniaturized antenna.....	34
2. Design two: Reconfigurable folded miniaturized antenna.....	38
3. Design three: New folded structure.....	42
4. Design four: New folded QGA structure.....	48
5. Design five: New folded reconfigurable QGA structure.....	54

F. Conclusion.....	57
V. SMALL ANTENNA MEASUREMENTS	59
A. Introduction.....	59
B. Small antenna measurement overview.....	59
C. Measurement of the various proposed designs.....	62
1. Design one: FMIoT measurement.....	63
2. Design three: FoMiP measurement.....	66
D. Conclusion.....	68
VI. CONCLUSIONS AND FUTURE WORK	70
REFERENCES	72

ILLUSTRATIONS

Figure		Page
1.	Biconical small Antenna [14].....	5
2.	Series and parallel RLC circuits. (a) Series RLC, (b) Parallel RLC [15].....	6
3.	Equivalence of some loaded antennas [13].....	7
4.	5-element MIMO antenna system for IOT and CR, (a) top view and (b) bottom view [28].....	9
5.	Antenna for paper [29].....	10
6.	Various techniques adopted to achieve reconfigurable antennas [31].....	11
7.	Categorization of Reconfigurable Antennas [32].....	11
8.	Pin diode-based frequency and radiation pattern reconfigurable antenna with the appropriate pin diode biasing network [33].....	13
9.	Front and back of the reconfigurable ‘‘Filtenna’’[34].....	13
10.	Tuning of the reflection coefficient of the ‘‘Filtenna’’ for different voltage levels[34].....	14
11.	A radiation pattern reconfigurable antenna [35].....	14
12.	MIMO systems based on PIN diode switch activated reconfigurable antennas[36].(a)Top layer,(b) Bottom layer.....	15
13.	An antenna with rectangular slots based on GA algorithm [43].....	19

14.	Infinitesimal connections and overlaps [41].....	19
15.	Antenna with dimensions chosen by GA [45].....	20
16.	Bloch sphere [52].....	24
17.	A typical representation of a quantum population [52].....	24
18.	Lookup table of the rotation angle [52].....	26
19.	Automation diagram for the GA.....	30
20.	Automation diagram for the QGA.....	32
21.	(a) 3D Folded antenna design (b) view of section2 (c) view of section 3.....	37
22.	The fabricated prototype of FMIoT.....	37
23.	Optimized position of the pin diode and the coax fed on the antenna...	38
24.	S-Parameter results of the ON state for FMIoT.....	39
25.	Realized gain of the ON state for FMIoT.....	39
26.	S-Parameter results of the OFF state for FMIoT.....	40
27.	Realized gain for the OFF state for FMIoT.....	40
28.	Fitness of the QGA.....	41
29.	Antenna and Current distribution	43
30.	S-parameter and realized gain.....	43
31.	Antenna and Current distribution on the antenna's patch.....	43
32.	S-Parameter and realized gain.....	44
33.	Antenna and Current distribution on the antenna's patch.....	44
34.	S-Parameter and realized gain.....	44
35.	Antenna and Current distribution on the folded antenna's patch.....	44

36.	S-Parameter and realized gain of the folded antenna.....	45
37.	Simple antenna design.....	45
38.	S-Parameter and realized gain of the simple antenna design.....	46
39.	Simple reconfigurable antenna design.....	46
40.	Reflection coefficient of the OFF state.....	47
41.	Realized gain on the OFF state.....	47
42.	Reflection coefficient of the ON state.....	47
43.	Realized gain of the ON state.....	48
44.	Antenna design using QGA.....	49
45.	Pixilation in the lower layer of the antenna.....	50
46.	Pixilation in the right layer of the antenna.....	50
47.	Pixilation in the left layer of the antenna.....	51
48.	Possible zone of the coax fed.....	52
49.	S-Parameter and realized gain of the QGA antenna.....	53
50.	Percentage of the fitness with respect to the number of iterations.....	53
51.	Fabricated prototype.....	53
52.	Reconfigurable QGA antenna design.....	55
53.	Percentage of the normalized fitness in function of the number of iterations.....	55
54.	S parameter in the OFF state.....	56
55.	Realized gain in the OFF state.....	56
56.	S parameter in the ON state.....	56

57.	Realized gain in the ON state.....	57
58.	Cross section of the dual-band balun prototype [64].....	60
59.	Ferrite beads and balun placed between the AUT and the cable for small antenna measurements [64].....	60
60.	Simulated and measured reflection coefficient of FMIoT.....	63
61.	The radiation pattern of FMIoT at 820 MHz in the (a) X-Z plane and (b) X-Y plane.....	63
62.	FMIoT antenna measurement using ferrite bead and a balun.....	64
63.	The prototype under measurement using a ballun and a ferrite bead.....	66
64.	Simulation and measurement of S-Parameters.....	66
65.	The radiation pattern of the antenna at 868 MHz in the (a) x-z plane and (b) y-z plane.....	67

TABLES

Table		Page
2.1.	Some miniaturizations techniques with their advantages and disadvantages.....	8
3.1.	Strategy of direction and size of rotation angle.....	20
4.1.	Frequency values for the ON and OFF states of the pin diode.....	41
4.2.	Comparison between different reconfigurable antenna designs of the thesis.....	58
5.1.	Measurement methods for small antennas with their accuracy.....	61
5.2.	Characteristics of some miniaturized antennas.....	64
5.3.	Characteristics of some miniaturized antennas.....	67

CHAPTER I

INTRODUCTION

A. Background and Motivation

The Internet of Things (IoT) platform requires the continuous connection between numerous compact devices. That connection is ensured by antennas that are integrated within the different devices. Such integration necessitates the miniaturization of the various antennas to satisfy size constraints. Different techniques are implemented to achieve miniaturization such as high dielectric constant materials, three-dimensional structural folding [1], slots and slits incorporation [2], in addition to resistive loading [3].

Many miniaturized antenna designs, proposed for IoT devices, are investigated in literature [2-5]. For example, in [2] slits and slots are introduced into the antenna structure for miniaturization purposes. The proposed miniaturized antenna reaches a size reduction of 37.73% by relying on slits that are added on both sides of the slot antenna. Furthermore, a reduction of 42.33% is achieved when the slits are on one side of the slot. Another miniaturized UHF monopole zigbee antenna is discussed in [4] and proposed for IoT devices' integration. The antenna relies on meandering techniques and shorting pins in order to achieve miniaturization. The combination of these techniques results in a non-uniform topology of the radiating element. The design achieves 50% size reduction in comparison to a simple monopole antenna that operates at 915 MHz. Furthermore, a compact printed antenna is discussed in [5] and proposed for WLAN/Zigbee/Bluetooth applications. The antenna is miniaturized by relying on

folding techniques. Such folding is done along the vertical axis (z-axis) of the structure. Further miniaturization of the antenna is also accomplished by resorting to folding along one of the horizontal axes (y-axis). As a result, the antenna reaches an 85% size reduction in comparison to a typical patch antenna.

On the other hand, several algorithms are used in antenna designs in order to further improve the antenna functionality such as particle swarm algorithm, genetic algorithm (GA), and quantum genetic algorithm (QGA). For example in [6], GA is used to determine the best configuration of the metal cells on the antenna structure in order to miniaturize the antenna. A miniaturization of 42% is achieved. Another design that resorts to GA in order to locate pixelated slots is discussed in paper [7] where a miniaturization of 37% is achieved. For example, in [8] particle-swarm optimization (PSO) algorithm is used in order to achieve an excellent performance for its tapered slot antenna. This PSO optimization reduces return loss, side lobes, and cross polarization below -18 dB and enables a symmetric circular beam. A VSWR < 1.6 and side lobes below -16 dB are also obtained.

QGA is characterized by high convergence rate, high accuracy and robustness. QGA can be employed to achieve many objectives. It is used for reconfigurable antenna optimization as discussed in [9], for antenna selection in massive MIMO systems as shown in [10], for broadband impedance and antenna tuning for multi-standard wireless communications as presented in [11], and to predict antenna radiation patterns from near-field measurements in a screened room. [12]

Merging the different techniques of miniaturization and different optimization algorithms is done in this thesis in order to determine the best and optimal miniaturized antenna designs. GA and QGA in addition to folding, slit, and slot loading are applied

on antenna structures in order to miniaturize them as well as to reconfigure their operation. The antennas are proposed to be integrated in IoT devices which govern their operational frequency to be centered at 868 MHz. In addition, these antennas must be able to provide Wi-Fi connectivity to the various devices, hence reconfiguration of frequency operation is proposed to enable a second operational mode at 2.4 GHz. Such frequency reconfiguration is accompanied by extreme miniaturization folds that reduce the size of the antenna without compromising its required radiation characteristics.

B. Thesis structure

The thesis is divided into 6 chapters. The first chapter is an introduction that identifies the general scope of this thesis report. Chapter II represents a general overview of antennas proposed for IoT integration. This chapter includes discussions about small antennas, miniaturization techniques, reconfigurable antennas and reconfiguration techniques. Chapter III discusses Machine Learning Algorithms applied on antenna structures. Chapter IV details the new antenna designs for IoT including the novel antenna structures, the different techniques used to create these designs, and the software tool as well as the fitness function developed in this thesis. Chapter V discusses small antenna measurement techniques, and displays the various measurement setups and results for the novel antennas (FMIoT and FoMiP antennas hereafter) proposed in chapter IV. Finally, chapter VI concludes this report and proposes potential future directions.

CHAPTER II

OVERVIEW OF ANTENNAS FOR IOT

A. Introduction

IoT is the interconnection of multiple devices allowing them to sense and to communicate. An important component used in IoT is the antennas. These antennas are used to ensure communication between the different devices. To be integrated in the IoT platform, the antennas should be miniaturized; in addition, they must be able to communicate at multiple frequencies, hence they should be reconfigurable. So, this chapter will start with an overview of electrically small antennas, then a discussion of miniaturization techniques will be done; in fact, many techniques can be used to achieve this miniaturization. In addition, an overview on different reconfiguration techniques and reconfiguration elements will be discussed.

B. Electrical small antennas

An electrical small antenna is an antenna that can be included in a sphere of radius a as shown in (Eq.1) [13]:

$$k \cdot a < 0.5, \text{ where } k = 2 \cdot \pi / \lambda \text{ (Eq.1) [13]}$$

This sphere is called the “Shu sphere” [13]. Small antennas present a challenge for antenna designers. In order to take advantage of the maximum possible space of the “Shu sphere” the use of volumetric form can be applied. Figure 1 shows the “Shu sphere” including an antenna [13].

In addition, the bandwidth of the antenna must fit the maximum bandwidth requirements engulfed by Geyi's formulas [14]. This formula is used to calculate the minimum quality factor (Eq.2) of the antenna design and the maximum acceptable bandwidth (Eq.3) where;

$$Q_{min} = \frac{1}{ka} + \frac{1}{2(ka)^3} \quad (Eq. 2)[14]$$

And

$$B_{max} = \frac{\text{Frequency [MHz]}}{Q_{min}} \quad (Eq. 3)[14]$$

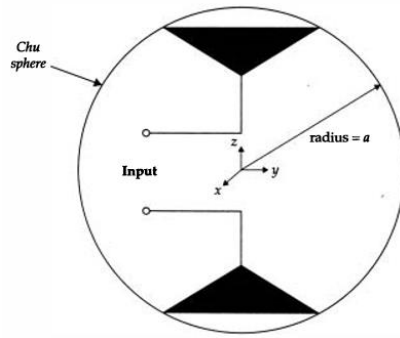


Figure 1: Biconical small Antenna [13]

C. Miniaturization techniques

1. Overview

In order to achieve electrical small antenna topologies, miniaturization techniques must be applied into the physical structure of the antenna. According to Wheeler [15], a small antenna in the TE_{10} mode corresponds to the RLC combination of Figure 2(a). The series capacitor is the ideal tuning element that takes the antenna to

resonance. Equally, a small antenna in the TM_{10} mode can be represented by the parallel RLC combination as in Figure 2b, where the shunt inductor is the tuning element that brings the antenna to resonance [15].

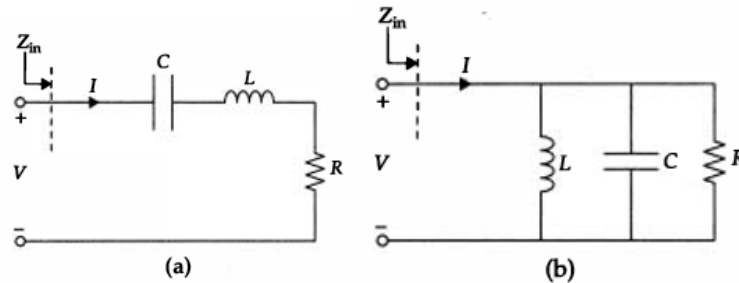


Figure 2: Series and parallel RLC circuits. (a) Series RLC, (b) Parallel RLC [15]

So applying both serial inductance and capacitance treatment maintains impedance matching and bandwidth. [13]

Such inductance and capacitance can be achieved by relying on lumped elements or by resorting to microstrip line technology. Ideally, lump components achieve miniaturization, but in reality they suffer from parasitic resistance. As a result of the accumulated resistance, the antenna's efficiency is significantly reduced. So the best way to increase the series inductance and shunt capacitance as well as achieve miniaturization is by relying on microstrip line technology and avoiding lump components to eliminate undesired parasitic effects.

Many miniaturization techniques are discussed in the literature. These techniques include the use of short-circuit elements [16], high dielectric constant material [17], slot incorporation [18], or resistive loading [19]. Although the most direct method for miniaturization is the use of high dielectric constant material, it can have a negative effect on the radiation efficiency [20] and results in a narrow bandwidth.

The use of a shorting wall can be applied to diminish the size of the antenna to $\lambda_0/4$ [21]. In addition, papers [22-23] discuss the use of shorting pins near the feed in order to diminish the size beyond $\lambda_0/4$. In paper [24], shorted pins are positioned between the upper patch and the ground plane in order to achieve a miniaturization.

Structural folding is another technique for antenna miniaturization. Modifying and optimizing the antenna's topology by bending certain parts, meandering integrated lines, or even incorporating volumetric curvatures, or fractal patterns contributes to the size reduction aspect of an antenna element. According to [25], a folded rectangular patch can decrease the resonant frequency by 50%.

Since folding the rectangular patch does not change its electrical length, the resonant frequency does not change, and the physical dimensions of the antenna decrease. As a result, miniaturization can be achieved by conserving the frequency of operation and decreasing the physical length of the antenna [26]

Slot loaded [13] patches can be represented by equivalent LC circuits as shown in Figure 3. When a slot is introduced, the surface currents in its vicinity are disturbed, resulting in an alteration of the inductance and capacitance values of the equivalent antenna impedance.

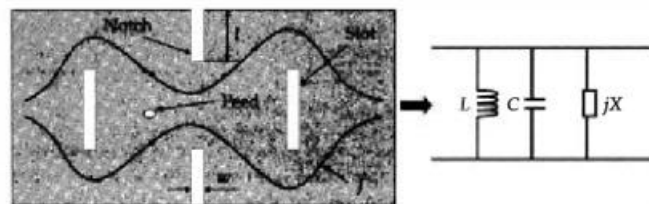


Figure 3: Equivalence of some loaded antennas [13]

Some of the miniaturization techniques with their advantages and disadvantages are summarized in the Table 2.1 [13].

Table 2.1: Some miniaturizations techniques with their advantages and disadvantages

[13]

Miniaturization	Use of	Advantages	Disadvantages
Miniaturized antenna	High dielectric substrate Magneto dielectric substrate	Easy to design	Limited bandwidth Expensive
Shorted antenna	Folding Shortening wall Shortening pins	Four-time miniaturization Effective solution	Non planer Complex geometry Low gain Low directivity No specific design steps
Slot loading	Fractal Slots in the patch	Eight-time miniaturization Wider bandwidth	Complex geometry No specific design steps Affects radiation characteristics

The radiation efficiency η is equal to the radiated power over the power delivered to the input as can be seen in Eq. 4, where R_{loss} denotes the loss resistance and R_{rad} denotes the radiation resistance. When the antenna size decreases the resistance loss R_{loss} increases, and the efficiency deteriorates.

$$\eta = \frac{P_{rad}}{P_{in}} = \frac{R_{rad}}{R_{rad} + R_{loss}} \quad (\text{Eq.4}) \quad [15]$$

2. Miniaturized antenna

In paper [28] a compact single-substrate planar multiband 5-element multiple input multiple output (MIMO) antenna system is presented. It is shown in figure 4. The antenna size is equal to $0.125\lambda_0$ by $0.046\lambda_0$. At the frequency of 0.8GHz, it gives a gain of -3.68 dB.

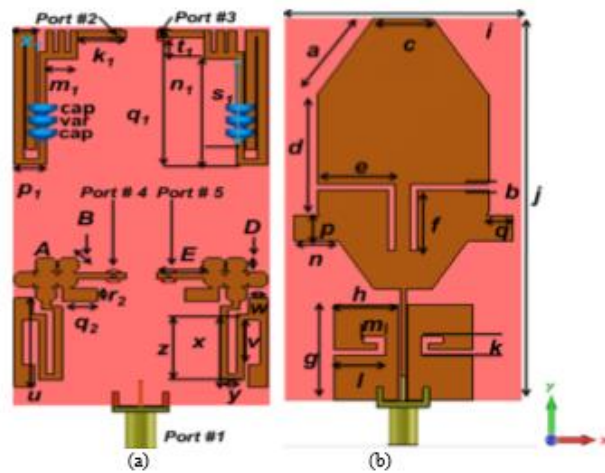


Figure 4: 5-element MIMO antenna system for IOT and CR, (a) top view and (b) bottom view [28]

An antenna for IoT having a size of $0.117 \lambda_0 * 0.057 \lambda_0$ is presented in [29]. This antenna is shown in figure 5, it operates at a frequency of 880MHz with a gain of -4.64 dB



Figure 5: Antenna for paper [29]

D. Reconfiguration

1. Overview

The reconfiguration of an antenna is obtained by changing the radiated fields of the antenna's effective aperture. [30] The reconfiguration is reached by introducing switches in the radiating surfaces of the antenna or in the feeding networks.

Many techniques can be used to create reconfigurable antennas. These techniques can be divided into four major categories: electrical, optical, mechanical, and material change. As shown in figure 6, the electrically reconfigurable antennas are based on RF-MEMS, PIN diodes, or varactors. In addition, optically reconfigurable antennas use photoconductive switching elements. On the other hand, physically reconfigurable antennas are created by mechanically changing the structure of the antenna. Reconfigurable antennas can also be created using smart materials such as ferrites and liquid crystals.[31]

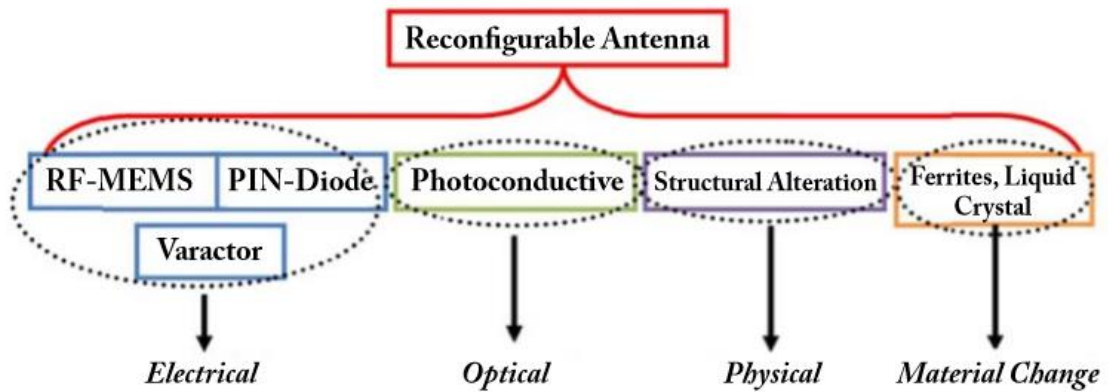


Figure 6: Various techniques adopted to achieve reconfigurable antennas[31]

Antennas can be divided into four groups as shown in figure 7. The first group includes frequency reconfigurable antennas. The second group includes radiation pattern reconfigurable antennas. The third group includes reconfigurable polarization antennas. And the fourth group includes reconfigurable antennas with hybrid reconfiguration techniques. [32]

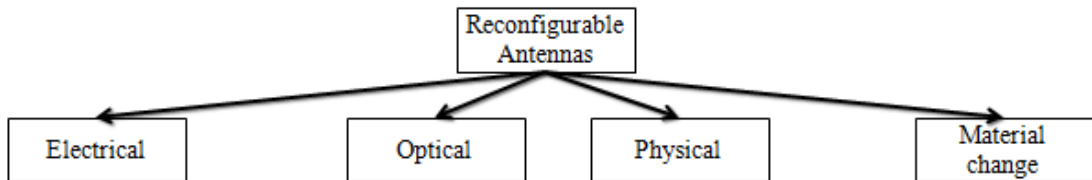


Figure 7: Categorization of Reconfigurable Antennas [32]

Different type of switches can be used to achieve reconfigurable antennas. Some of these switches include RF MEMS, pin diodes, and varactors. RF MEMS create a short or open circuit in the surface current paths of the antenna structure. PIN Diodes have two different states; the “ON” and the “OFF” state. The diode is forward biased in the “ON” state, the diode is not biased or is reverse biased in the “OFF” state. Varactors consist of a p-n junction diode; when the biased voltage on the diode changes, the capacitance of the varactor changes and thus tunes the antenna operation[31].

In addition, each switch is characterized by some properties [30]; RF MEMS are characterized by their high isolation and low power. Pin diodes necessitate a constant DC current, and they are characterized by their fast switching characteristic. Varactors necessitate a direct supply of a DC voltage; they are characterized by their fast switching characteristic and their tunable response. Optical switches do not require biasing and they are characterized by their high isolation.

Alternative (non-switch) based techniques can be used to achieve reconfiguration. These techniques use some tools to move some parts in the antenna structure or change the electrical properties of the antenna's substrate. Reconfiguration properties and techniques must be specified at the beginning of each design process.

2. Reconfigurable antenna

Many challenges can be faced while designing reconfigurable antennas; in fact, many factors must be considered. Reconfigurable antennas must achieve a good gain, stable radiation, and a good impedance matching on the various operating states of the antenna. [30]

A reconfigurable antenna using pin diodes is discussed in paper [33]. The antenna is composed of two monopoles at an angle of 30 degrees from each other. A reflector is allocated in the middle of the two monopoles in order to achieve pattern diversity. The two monopole arms are connected to a tapered feeding line by two pin diodes. When one of the two switches are activated, the antenna resonates at the frequency of 3.24 GHz. Two additional pin diodes are added on the monopoles in order

to increase its length. That increase in the length results in a decrease in the resonant frequency to 2.96 GHz. The antenna is shown in figure 8.

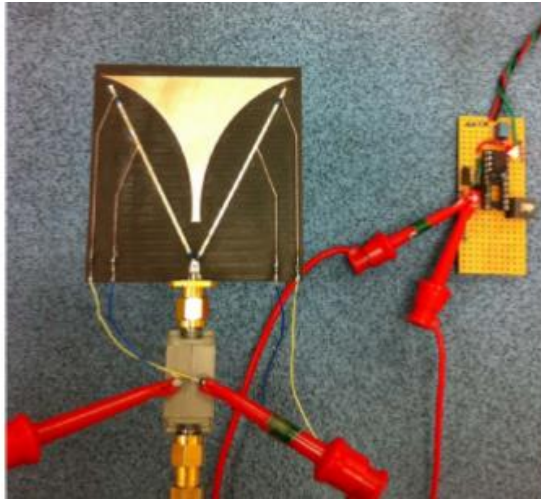


Figure 8: Pin diode-based frequency and radiation pattern reconfigurable antenna with the appropriate pin diode biasing network [33]

Another reconfigurable design [34] is a varactor based reconfigurable filtenna shown in figure 9.

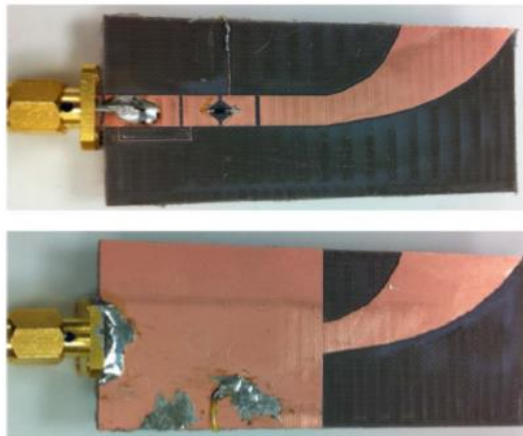


Figure 9: Front and back of the reconfigurable ‘Filtenna’[34]

In fact, a ‘Filtenna’ describes a filter combined in the feeding line of an antenna. A varactor tunable filter is introduced in the feeding line of a printed antipodal wideband dipole antenna. This merging results in a frequency tuning without altering

the radiation characteristics of the antenna. The tuning of the reflection coefficient of the ‘‘Filtenna’’ for different voltage levels is shown in figure 10. [34]

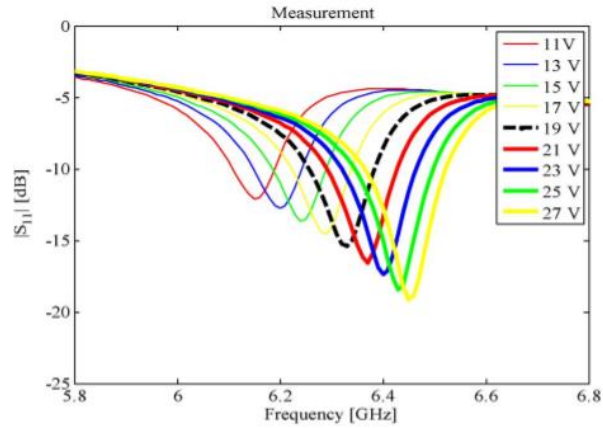


Figure 10: Tuning of the reflection coefficient of the ‘‘Filtenna’’ for different voltage levels[34]

A reconfigurable rectangular spiral antenna is shown in figure 11, where RF-MEMs switches are integrated in the antenna structure. The antenna is composed of five sections. These sections are connected through four RF-MEMS switches. According to the status of the RF-MEMS, the antenna can change its radiation beam direction.[35]

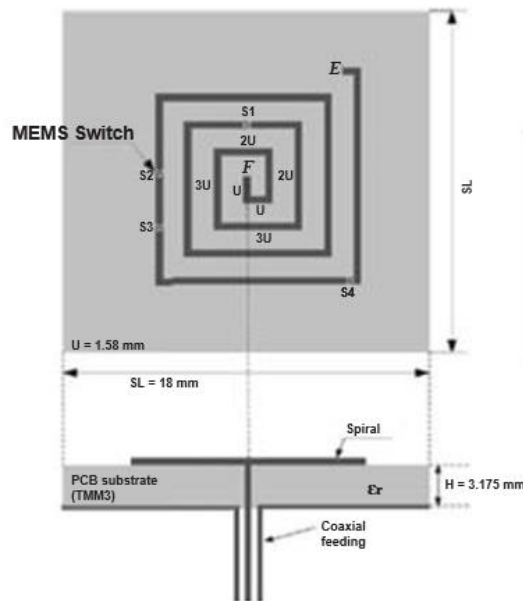


Figure 11: A radiation pattern reconfigurable antenna [35]

Paper [36] describes two reconfigurable antennas using PIN diodes, these antennas form a MIMO system operating over a wide-bandwidth with notch frequency reconfiguration. The antennas are shown in figure 12.

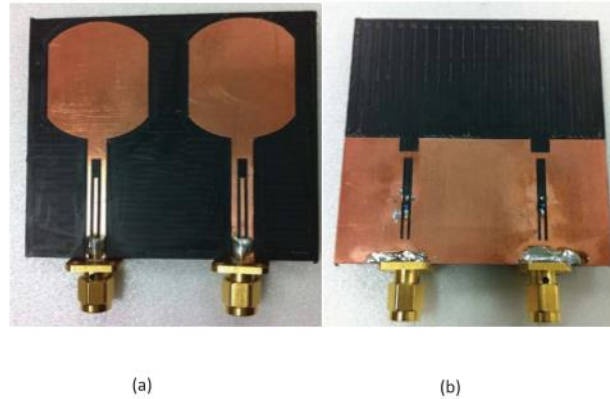


Figure 12: MIMO systems based on PIN diode switch activated reconfigurable antennas[36].(a)Top layer,(b) Bottom layer.

E. Conclusion

This chapter introduces IoT concepts, it presents a background on small antennas, and on antenna miniaturization; in fact, many techniques can be applied to reach this miniaturization. Some of these techniques are based on folding the antenna structure, relying on material with high dielectric constants, integrating shorting walls, incorporating shorting pins, as well as loading the patch with slots. In fact, miniaturization affects the radiation efficiency, the bandwidth and the gain. As a result, the design of an antenna must be a compromise between its size and its performance.

In addition, this chapter presents an overview on reconfigurable antennas with the different techniques of reconfiguration and different types of switches used. It details some examples of reconfigurable antennas done in the literature.

CHAPTER III

MACHINE LEARNING ALGORITHMS APPLIED ON ANTENNA STRUCTURES

A. Introduction

Machine learning can be used as an optimization tool in antenna design when a certain degree of complexity is required in the structure. In fact, many algorithms can be used for such an optimization. GA is one of the most popular and widely used evolutionary algorithms (EA). QGA is an improvement of GA with better performance because it introduces some thoughts of quantum computing into GA which greatly improves the parallelism of genetic manipulation, and accelerates the convergence process; in addition, QGA is characterized by high convergence rate, high accuracy and robustness [37].

This chapter starts with an introduction on GA and gives some examples on the implementation of GA for antenna designs. Then it discusses QGA with some of the relevant literature review about this topic.

B. Genetic Algorithm

1. Overview

GA is described as a search algorithm. It works on a set of elements, called population. This population will progress through crossover and mutation, towards a maximum of the fitness function. [38]

GA is a method based on the principles of natural [39] selection and evolution. It is a stochastic pursuit algorithm. GA employs biological concepts like chromosomes, genes, alleles, mating, and mutation. In GA the fitness function plays a crucial role in optimization. This fitness function must be designed in a way to find the optimized solution with the best efficiency, bandwidth and gain.

The most important steps in the GA algorithm beyond the fitness function are the 1) Initialization where the GA generates an initial population of random population, 2) Selection where the parents producing the next generation are selected [40]. The probability of a parent being selected depends on its fitness value. Some types of selection are tournament and roulette wheel selection. Crossover exchanges segment of bits between pairs of chromosomes. Crossover is specified by the developer and can be at single or multiple locations. Finally, Mutation randomly changes one or more bits.

2. Antenna design using GA

GA optimization is used for in antenna design optimization. According to [41], a simple rectangular patch antenna is divided into 63 cells. Each of these cells represents a conducting or non-conducting element. To represent these cells in the GA algorithm a binary coding is done with 63 bits. Five genes indicate the feed position, and five more genes are added for the shorting pin. The fitness function was determined as the

summation of reflection coefficients in each of three bandwidths divided by ten times the total number of samples.

In each generation the number of chromosomes in each population is 20. The mutation rate is taken to be 60%. And the method used for selection is the tournament selection method. According to [41], if all possible solutions were generated, 2^{63} possible geometries will be achieved.

In [42], a dual-band antenna is designed and used for ground based and airborne based systems. The parameters used for training were extracted from AED and then evaluated by the fitness function. Patch surface was divided into 46 binary cells. Half of the patch was designed, so a symmetric condition beside the E-plane was reached for the purpose of reducing the cross-polarization component. 200 generations are specified with 260 chromosomes with the tournament selection method. Difference between the simulated results and the measured ones was caused due to imprecision during manufacturing.

An electromagnetic GA optimization (EGO) is proposed in [42]: it combines the robustness of GA with the precision of AED and the quickness of parallel calculating. The designed antenna displayed acceptable dual-band operation at the frequencies of 1.9 and 2.4 GHz, while keeping a cross-polarization level of 11 dB below the cross-polarization maximum. Furthermore, some designs necessitate binary and non-binary inputs. The real part represents the dimensions, and the binary part represents the slots, as can be seen in the figure 13. [42] uses the hybrid PSO for the optimization. While designing the antenna, the designer should be able to choose the geometry of the antenna in addition to tuning the parameters in order to achieve the desired goal. A binary GA and binary PSO strings are generated. However, since using continuous

values and mapping them to binary is very costly, a solution would be to crossbreed both the real and binary elements into one chromosome. This hybrid technique gave high quality performance. The results display that 40% bandwidths are attained at required frequencies ranges, in addition to S11 value of -20dB at the frequency of 1.8GHz and S11 value of -13 dB at the frequency of 2.4GHZ. However, these results needed a minimum of 200 iterations.[43]

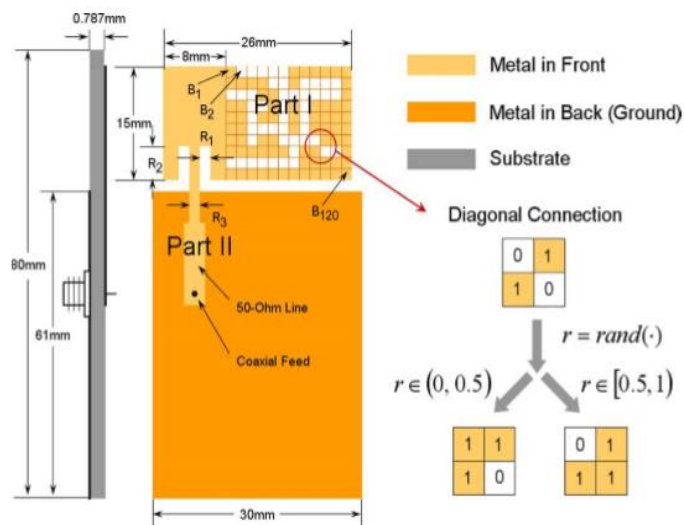


Figure 13: An antenna with rectangular slots based on GA algorithm [43]

Furthermore, an important problem that we can face while applying this conducting and non-conducting element process [41] is the presence of infinitesimal connections that ruins the simulation. A solution that can be applied is the use overlapping cells. So, a robust manufacturing can be reached. This technique is shown in figure 14.

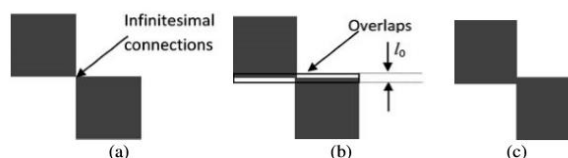


Figure 14: Infinitesimal connections and overlaps [41]

In addition, a GA optimization can be used to minimize the resonant frequency of a rectangular patch antenna without changing its size [44]. In paper [44] and after the optimization, the resonant frequency is reduced from 3 to 1.8 GHz. The patch was divided into 9 by 9 squares cells. This patch antenna is fed by a probe, so all cells can be 0 or 1 except the cell of the probe which must always be 0. Chromosomes are selected randomly. The method used for selection is tournament and the cross over is a single point cross over. The cycle repeats itself for a certain determined number of iterations. A start and end frequency in addition to the number of frequencies are selected for each iteration. For each frequency predefined S11 is measured. The frequency having the lowest S11 is selected. Then the cost function is the difference between the desired frequency and the obtained frequency. A reduction of 42 % is achieved in resonant frequency.

Another example of using GA for antenna optimization is presented in [45], where a microstrip patch antenna is designed; the GA is used to regulate the ideal dimensions of the antenna for its best performance as shown in figure 15.

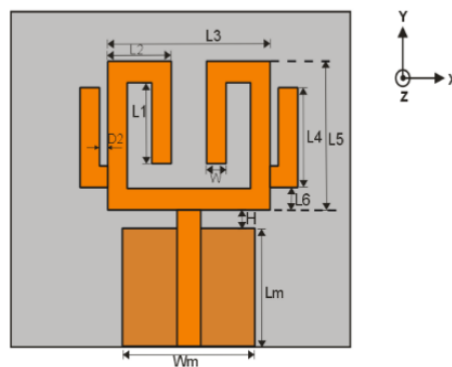


Figure 15: Antenna with dimensions chosen by GA [45]

The dimensions of the antenna are chosen randomly, and a certain range of allowed values is defined for each dimension. Since this antenna operates at 3 frequencies, they are included in the fitness function with three different weights.

The population is formed of 64 chromosomes and the number of generations is set to 20. The probability of mutation is defined as 0.06. The best possible configuration is reached where at frequency 2.4 GHz the reflection coefficient is -25 dB, at 3.6 GHz the reflection coefficient is -37 dB and at 5.5 GHz the reflection coefficient is -14 dB.

Furthermore, paper [40] presents the design of a single and dual polarization PIFA antenna optimized by the GA algorithm. When changing the length of the patch and the position of the shorting pin the antenna configuration changes. The S11 is taken in consideration for the evaluation of the design. Choosing the frequency of operation for the best reflection coefficient in each band of frequency is a hard task. So the optimization techniques are the best solution for this problem.

The initial population is randomly generated; this population is formed of the length of the microstrip, the position of the port, and the position of shorting pin. The fitness used is the minimum of S11. After optimization the reflection coefficient at the frequency of 2.4 GHz reached approximately -35 dB which is a very good matching. The fabricated antenna gives slightly different values and that is due to error in fabrication.

To achieve the optimization, the combination of the GA algorithm and AED can be applied [46]. The technique is realized using MATLAB. The goal is to design a broadband E-shaped microstrip antenna. The dimensions of the patch (including its length, width, and the height of the substrate), the coordinates of the position of the

probe, and the dimensions of the two parallel slots etched in the patch must be optimized. The population size is 50, with 200 iterations.

N is the number of frequencies to be considered, S11 the reflection coefficient. After approximately 24 iterations the best fitness improves to reach 1, so the goal was reached.

Sometime the goal is not to reach the optimal value but an acceptable one. Paper [47] presents a microstrip antenna used in medical implants. GA algorithm is used for the design of this antenna. Each chromosome was formed of 320 bits, the first 300 bits represents the cells of the patch and the last 20 bits represents the location of the feed and the location of the ground. The simulation of each model takes more than 30 minutes. When the requirement is met the process is terminated. The convergence of a larger antenna is faster than that of a smaller antenna. Good designs were reached after approximately 20 generations. These results were not the optimal ones, but they met the requirement conditions.

Finally, some designs are very complex to evaluate. For example, the design of an Elliptical microstrip patch antenna is very complex. So, the proportions of the elliptical microstrip patch antenna are designed using GA. GA algorithm is a better approach than ANN because no training of the data is necessary. The unknown parameter is the semi major axis. 20 individuals form the population, 200 generations are formed, the crossover probability is fixed to be 0.2, and the mutation probability is 0.01. The obtained reflection coefficient for the frequency of 1 GHz was -19 dB. By using GA in optimizing the designs, the difficulty of the design of the elliptical antenna was eliminated. [48]

GA is one important method for miniaturization; it can search for the best position for the slot on a patch. The fitness function is the most important part in the GA. This fitness function helps in the convergence of the algorithm on the best possible solution.

C. Quantum Genetic Algorithm

1. Overview

GA has a slow convergence speed, and it is subjected to a local optimal solution. QGA introduced some thoughts of quantum computing into GA, which greatly improved the parallelism of genetic manipulation and accelerated the convergence process [49]. In addition, QGA is characterized by high convergence rate, high accuracy and robustness.

Every bit of gene in the chromosomes of each population is encoded in the form of Q-bit[50]. The Q-bit illustration for the chromosomes of the population is a necessary point for applying the quantum algorithm. By implementing a Q-bit chromosome representation, a classical population can be produced by continually measuring the quantum population. The best elements of each population are used to update the quantum population [51]

A Q-bit is the simplest quantum system. It is the fundamental unit. Q-bit has 2 special states, these states are $|0\rangle$ and $|1\rangle$ (Eq.5). Upon measurement, a Q-bit loses its quantum character and reduces effectively to a bit. [52]

The Bloch sphere is a geometrical representation of the Q-bit shown in figure 16. With:

$$|\psi\rangle = a|0\rangle + b|1\rangle \text{ (Eq.5) [52]}$$

Where

$$|a|^2 + |b|^2 = 1 \text{ (Eq.6)}$$

The north and south poles of the Bloch sphere are typically chosen to correspond to the standard basis vectors $|0\rangle$ and $|1\rangle$.

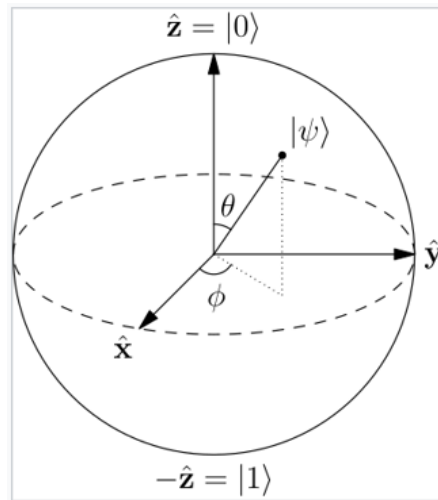


Figure 16: Bloch sphere [52]

Each quantum individual XQ in the quantum population, Q-pop, is generally represented as a quantum register. Figure 17 represents a typical representation of a quantum population.

$$\begin{array}{l} \vec{XQ}_1 \left[\begin{array}{c|c|c|c|c|c} \alpha_{1,1} & \alpha_{1,2} & \alpha_{1,3} & \alpha_{1,4} & \cdots & \alpha_{1,d} \\ \beta_{1,1} & \beta_{1,2} & \beta_{1,3} & \beta_{1,4} & \cdots & \beta_{1,d} \end{array} \right] \\ \vec{XQ}_2 \left[\begin{array}{c|c|c|c|c|c} \alpha_{2,1} & \alpha_{2,2} & \alpha_{2,3} & \alpha_{2,4} & \cdots & \alpha_{2,d} \\ \beta_{2,1} & \beta_{2,2} & \beta_{2,3} & \beta_{2,4} & \cdots & \beta_{2,d} \end{array} \right] \\ \vdots \\ \vec{XQ}_N \left[\begin{array}{c|c|c|c|c|c} \alpha_{N,1} & \alpha_{N,2} & \alpha_{N,3} & \alpha_{N,4} & \cdots & \alpha_{N,d} \\ \beta_{N,1} & \beta_{N,2} & \beta_{N,3} & \beta_{N,4} & \cdots & \beta_{N,d} \end{array} \right] \end{array}$$

Figure 17: A typical representation of a quantum population [52]

QGA includes the initialization part, the selection, quantum crossover, quantum mutation, and quantum interference, quantum measurement, evaluation and replacement.

In QGA, during the population initialization, all the probability amplitudes of chromosomes are initialized with $1/\sqrt{2}$. That means each chromosome has the same probability in all possible linear superposition states.

2. *Quantum gate*

In the quantum interference part, a perturbation mechanism called Q-gate is used. It is applied to each produced quantum offspring and parent. It amplifies the amplitudes of having the best solution and consequently decreases the amplitudes of having other solutions. So, the quantum interference encourages better search for the best solutions. [52]

The quantum gate is an operation mechanism to complete the evolution. It is chosen following specific problems. Many kinds of quantum gates exist. Population can be updated through quantum gate as shows the equation below. The quantum gate used in (Eq.7) is the rotation gate, where Θ_i is the rotation angle, its size and corresponding symbols are determined by the original design adjustment strategy shown in table 3.1. The probability amplitudes are $[\alpha_i \beta_i]$ and $[\alpha_i' \beta_i']$ [53]

$$\begin{bmatrix} \alpha_i' \\ \beta_i' \end{bmatrix} = U(\theta_i) \begin{bmatrix} \alpha_i \\ \beta_i \end{bmatrix} = \begin{bmatrix} \cos \theta_i & -\sin(\theta_i) \\ \sin(\theta_i) & \cos \theta_i \end{bmatrix} \begin{bmatrix} \alpha_i \\ \beta_i \end{bmatrix} \quad (\text{Eq.7}) \quad [53]$$

Table 3.1: Strategy of direction and size of rotation angle [53]

x_i	$best_i$	$f(x) > f(best)$	$\Delta\theta_i$	$s(\alpha_i, \beta_i)$			
				$\alpha_i, \beta_i > 0$	$\alpha_i, \beta_i < 0$	$\alpha_i = 0$	$\beta_i = 0$
0	0	FALSE	0	0	0	0	0
0	0	TRUE	0	0	0	0	0
0	1	FALSE	$\Delta\theta_i$	+1	-1	0	± 1
0	1	TRUE	$\Delta\theta_i$	-1	+1	± 1	0
1	0	FALSE	$\Delta\theta_i$	-1	+1	± 1	0
1	0	TRUE	$\Delta\theta_i$	+1	-1	0	± 1
1	1	FALSE	0	0	0	0	0
1	1	TRUE	0	0	0	0	0

Several Q-gates are used in the literature. These Q-gates are represented as matrices, where the number of input Q-bits is equal to the number of outputs Q-bits. The rotation gate acting on a single Q-bit is the basic Q-gate in quantum-inspired algorithms. Figure 18 represents a lookup table of the rotation angle in the rotation Q-gate.[52]

Other gates include the Pauli-X gate, Pauli-Y gate, Pauli-Z gate, Square root of NOT gate, Phase shift gates, swap gate, Square root of Swap gate, Controlled gates (CNOT), Toffoli (CCNOT) gate, Fredkin (CSWAP) gate, and Ising gate.

α	β	Reference bit value	Rotation angle
>0	>0	1	$+\Delta\theta$
>0	>0	0	$-\Delta\theta$
>0	<0	1	$-\Delta\theta$
>0	<0	0	$+\Delta\theta$
<0	>0	1	$-\Delta\theta$
<0	>0	0	$+\Delta\theta$
<0	<0	1	$+\Delta\theta$
<0	<0	0	$-\Delta\theta$

Figure 18: Lookup table of the rotation angle [52]

3. QGA applications

Applications of quantum computation are used in multiple areas. QGA are used for feature selection [54], for handling probabilistic, interval, and fuzzy uncertainty [55]. In addition, QGA can be employed to achieve many objectives. It is used to design reconfigurable antennas, by optimizing the position of the switches [9]. QGA is also used for antenna selection in massive MIMO systems as shown in [10]. QGA is applied for broadband impedance and antenna tuning for multi-standard wireless communications as presented in paper [11]. QGA is used to predict the antenna radiation patterns from near-field measurements. [12]

D. Conclusion

This chapter gives an overview about GA and QGA which is an improvement of GA with better performance. In fact, this chapter discussed some application done in literature using both algorithms.

CHAPTER IV

NEW ANTENNA DESIGNS FOR IOT

A. Introduction

In this thesis, various software codes are written to assist in the design of antennas specific for IoT integration. MATLAB [56], Ansys Electronics Desktop (AED) [57] and VBScript [58] are used simultaneously to generate automated codes. This chapter introduces the automation codes using GA and QGA. Two fitness functions are created; one is used to design miniaturized antennas, and the other one is used to reconfigure such miniaturized structures. These fitness functions are also be discussed in this chapter. The different designs created in this thesis are detailed in the final part of this chapter.

B. Automation part

AED uses a scripting language called VBScript which is a Microsoft® Visual Basic® Scripting Edition in order to record macros. Since scripts are known to be fast and effective, they present suitable solutions to complete repetitive tasks. The script is formed of multiple commands, which will be executed simultaneously throughout the execution of the code. The script can be written as a code on a text editor and then can be run in AED, or the script can be recorded from AED into a text editor, where it can be modified and then run in AED. The text editor can later be accessed, and the code modified whenever necessary. [59]

C. MATLAB code for automation

As a first step, a folded antenna is designed. A VBSCRIPT code of the created folded antenna is written. The next step is based on miniaturizing the folded antenna. Optimization techniques are used for that purpose.

1. GA automation code

A GA is applied to the folded antenna structure. The GA is written as a MATLAB code. A population of 20 chromosomes is generated. For the initialization part of the GA, a random population of chromosomes is generated. Selection, crossover and mutation are applied to the chromosomes. The mutation rate used is 20% in order to decrease the probability of convergence to a local optima. A MATLAB code maps the different chromosomes of the population into different VBSCRIPT codes. The different bits of the chromosomes represent the position of the slots on the antenna patch in addition to the location of the coax fed. For the reconfigurable antennas, more bits are added to the chromosome to represent the location of the switch.

The different VBSCRIPT codes create different antenna designs. These designs are run in AED. At the end of simulations, the results (Frequency, gain, and S11) are extracted into excel files.

The MATLAB code reads the results of all the chromosomes in the population from the excel files. A fitness function evaluates these results. The best 50% of the chromosomes are kept. Parts of the chromosomes will be discarded, and others will be

conserved. The GA algorithm is rerun based on the new results. These steps are repeated until convergence is achieved.

The complementary use of MATLAB, VBScript, and AED for optimization economizes time and is very advantageous. It transforms the process into an automated and efficient one. The different steps of this automation are presented in figure 19.

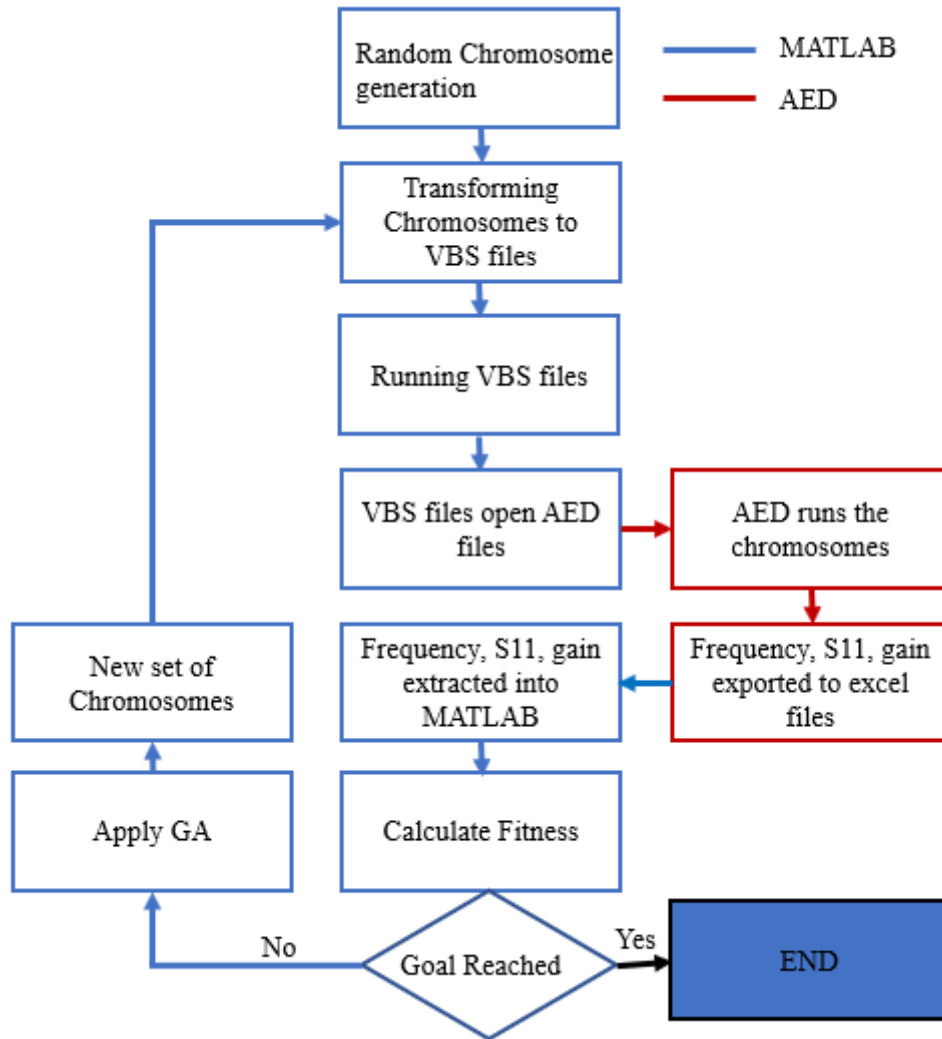


Figure 19: Automation diagram for the GA

2. QGA automation code

A QGA algorithm is applied to the folded antenna structure. The QGA algorithm is also written as a MATLAB code.

A population of 20 chromosomes is generated. For the initialization part of the QGA a quantum population of value $\frac{1}{\sqrt{2}}$ of chromosomes is generated. The quantum population is mapped into a binary population using a random pick. Then a quantum rotation gate is used.

A MATLAB code maps the different chromosomes of the population into different VBSCRIPT codes. The different bits of the chromosomes represent the position of the slots on the antenna patch in addition to the location of the coax fed. For reconfigurable antennas, more bits are added to the chromosome to represent the location of the switch.

The different VBSCRIPT codes create different antenna designs. These designs are run in AED. At the end of the simulations, the results (Frequency, gain, and S11) are extracted to excel files.

The MATLAB code reads the results of all the chromosomes in the population from the excel files. A fitness function evaluates these results. The best chromosome is saved.

The complementary use of MATLAB, VBScript, and AED for optimization is very useful and saves time. It transforms the process into an automated and efficient one. The different steps of this automation are presented in figure 20.

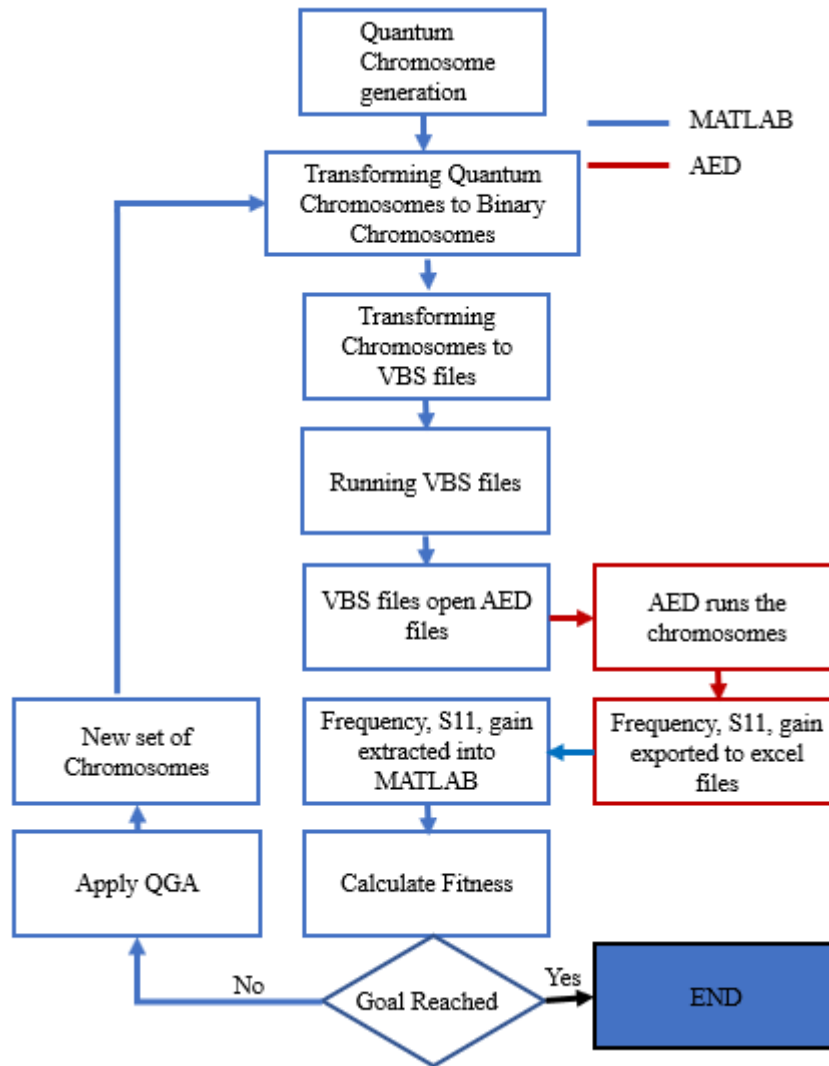


Figure 20: Automation part for the QGA

D. Fitness function

The fitness function is an important element in the process of convergence of the algorithm.

Some of the parameters that must be taken in consideration to ensure good antenna design are the frequency of operation, the gain and the S-parameter of the

antenna. The fitness function must include these three main factors in order to be optimized.

In this report we develop two different fitness functions; one for the simple design and the other for the reconfigurable one.

1. Simple fitness

As shown in equation 8, the cost function must increase with the increase of the difference between the frequency of operation and the desired frequency (0.868 GHz). In order not to obtain a cost value of zero when we reach the desired frequency of 0.868 GHz, a value of 1 is added to the numerator.

$$\text{cost} = \frac{1}{\text{fitness}} = \frac{(10 * (\text{abs}(\text{Frequency}) - 0.868) + 1)}{\left(\exp\left(\frac{\text{Gain}}{4}\right)\right) * \text{abs}(S_{11})} \quad (\text{Eq. 8})$$

In addition, the cost must increase with the decrease of the absolute value of S_{11} ; so the absolute value of reflection coefficient is inversely proportional to the cost and must be included in the denominator.

Furthermore, the cost must decrease when the gain is positive and increasing, and the cost must increase when the gain is negative and increasing. As a result, the positive gain and the cost are inversely proportional, and the negative gain and the cost are proportional. As a result, the exponential of the gain is put in the denominator.

2. Reconfigurable fitness

In addition, another fitness function was developed for the reconfigurable design (Eq.9). In fact, two entities are added in order to form the new cost function. One entity represents the ON state, and the other the OFF state. The cost function is as follows.

$$cost = \frac{1}{fitness} = \frac{(10 * (abs(frequencyON) - 0.868) + 1)}{((\exp(\frac{gainON}{4})) * abs(S11ON))} + \frac{(10 * (abs(frequencyOFF) - 2.4) + 1)}{((\exp(\frac{gainOFF}{4})) * abs(S11OFF))}$$

(Eq. 9)

E. Antenna designs

Our thesis objective is divided in two parts. The first part defines the functionality of the antennas. The antennas are proposed to be integrated in IoT devices which govern their operational frequency to be centered at 868 MHz. In addition, these antennas must be able to provide Wi-Fi connectivity to the various devices; hence reconfiguration of frequency of operation is proposed to enable a second operational mode at 2.4 GHz.

The design objective is to then design the antennas according to the RF theory principles. Optimization algorithms will be later added in order to reach the best optimal design solution.

1. Design one: Folded miniaturized antenna

Our first antenna was designed by applying miniaturization techniques on a regular patch antenna. The first step consists of designing a typical patch antenna that exhibits total dimensions of $52 \times 30 \text{ mm}^2$; operating at 2 GHz. Folding is later applied on the antenna as shown in Figure 21 to decrease the overall dimensions of the design while maintaining the same frequency of operation [26]. As a result, the dimensions of the antenna are minimized to $30 \times 31.84 \text{ mm}^2$ with a height of 4.37mm. To reach the desired frequency band (805-835 MHz), slots, slits and shorting pins are inserted into the design. Four slits and three slots are etched from section 2 of the antenna and two slits with one slot are etched from section 3 as shown figure 21. The position of the slits and slots were determined where the current distribution is the highest on the patch of the antenna. In addition, two shorting pins are incorporated in section 3 to ensure impedance matching at the desired frequency of 820 MHz.

As a result, a novel miniaturized antenna with a 95 % size reduction and a radiation efficiency 55% is designed to operate at 820 MHz [60]. The proposed design is a folded miniaturized antenna for IoT (hereafter FMIoT). This antenna is suitable for IoT devices' integration [6] because it targets the IoT Europe band (805-835 MHz). As shown in Figure 21, this antenna is composed of seven components that constitute the complete antenna structure. The antenna forms a three dimensional (3D) folded patch structure. Three layers represent its structure. The first layer is the radiating patch, the second layer is the Rogers Duroid Substrate 5880 with a dielectric constant of 2.2 and a thickness of 0.79 mm. The third layer is the ground plane that is covering the bottom layer of all sections.

The different parts of the antenna are fabricated using a mechanical milling machine and the different parts are soldered together in order to form the 3D shape.

Figure 22 shows the fabricated prototype of the antenna design. The parameters of the FMIoT are measured. The reflection coefficient is measured by relying on a vector network analyzer. The antenna is considered a miniaturized antenna by referring to the “Shu Sphere” theorem, [13]. The “Shu Sphere” theorem states that an antenna is considered miniaturized if it can be included in a sphere of radius a as shown in Eq. 1

$$k * a < 0.5 \text{ (Eq.1)}$$

In this design, the antenna can be engulfed by a sphere of diameter equal to 41.85 mm. As a result,

$$k * a = 0.36 < 0.5$$

In addition, the bandwidth of the antenna (30 MHz) fits the maximum bandwidth requirements engulfed by Geyi's formulas [14]. This formula is used to calculate the minimum quality factor (Eq.2) of the antenna design and the maximum acceptable bandwidth (Eq.3) where;

$$Q_{min} = \frac{1}{ka} + \frac{1}{2(ka)^3} = 13.5 \text{ (Eq.2)}$$

And

$$B_{max} = \frac{\text{Frequency [MHz]}}{Q_{min}} = 60.7 \text{ MHz (Eq.3)}$$

As a result, our first objective was achieved; in fact, we were able to design a miniaturize antenna that can be integrated in an IoT platform. Our next objective is reconfigurable which will make this antenna able to operate on another frequency of 2.4 GHz in order to provide WIFI connectivity. To achieve this reconfiguration, switches must be added in the radiating surfaces of the antenna, as a result the radiated fields of the antenna's effective aperture will change. So in the following design one kind of

electrical switches called pin diode will be used to achieve reconfiguration. A problem that presents itself is how to find the optimal position of the pin diode on the antenna. In the following, GA and QGA algorithms will be used in order to find this optimal position.

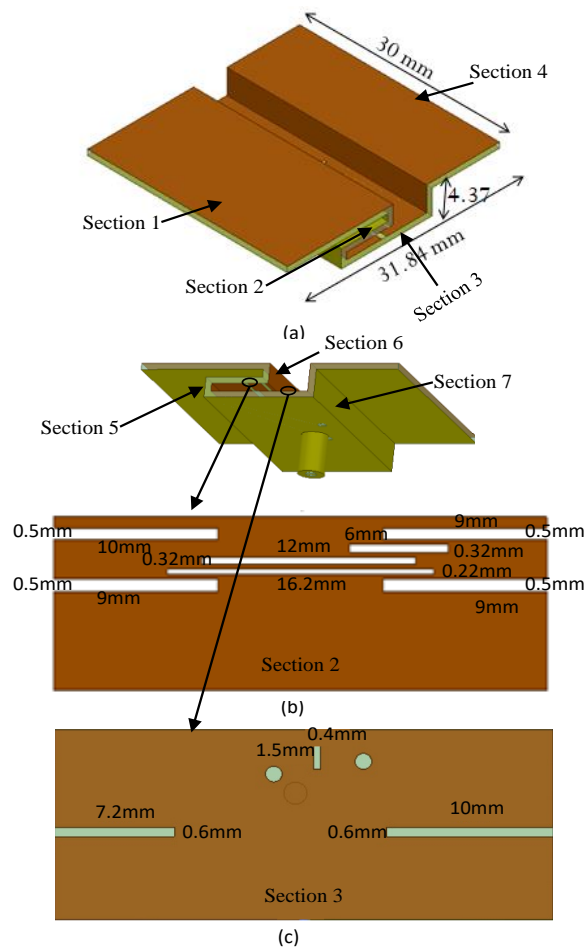


Figure 21: (a) 3D Folded antenna design (b) view of section2 (c) view of section 3



Figure 22: The fabricated prototype of FMIoT

2. Design two: Reconfigurable folded miniaturized antenna

GA optimization is first employed in order to reconfigure the frequency operation of the FMIoT, by relying on a single PIN diode. The GA identifies through rigorous optimization, the best position for the placement of the pin diode as well as one of the shortening vias. The ground plane on the upper layer is extended in order to appropriately bias the PIN diode as shown in figure 23.

In the GA code, the upper layer of the antenna is divided into 300 bits. These bits represent the possible locations of the pin diode. In addition, the position of one of the vias must be optimized in order to ensure matching. 100 bits of the chromosome represent the possible location of the via. It is important to note that crossover is also applied to the chromosomes with a mutation rate of 20%. Selection is done by relying on a Roulette Wheel selection technique.

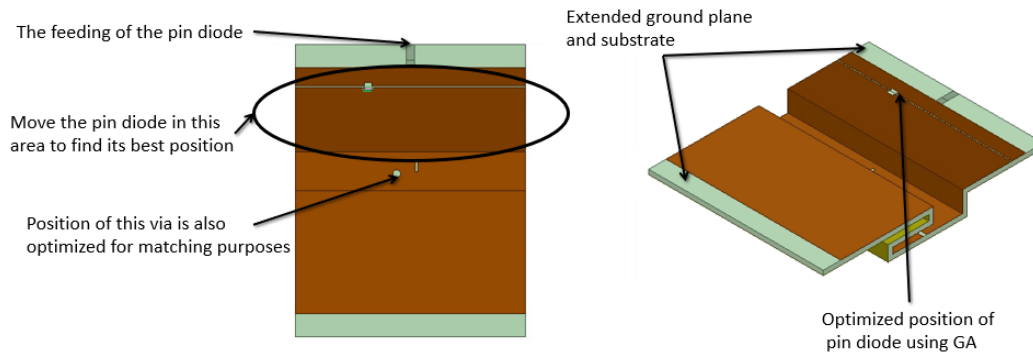


Figure 23: Optimized position of the pin diode and the coax fed on the antenna

The GA converged after 10 iterations on a local optima. The resulting antenna structure is shown in figure 23.

For the ON state of the pin diode, a resonance at around 0.8775GHZ with a magnitude of the reflection coefficient of -21 dB and a realized gain of around -4.81259

dB is achieved. Figure 24 shows the simulated reflection coefficient at 0.8775 GHz, and figure 25 shows the realized gain of the antenna. For the OFF state of the pin diode the simulated reflection coefficient indicates a resonance at around 1.74 GHz. In addition, the resulting realized gain is around -2.23747 dB. Figure 26 displays the simulated the reflection coefficient for the off state of the PIN diode, figure 27 displays the realized gain of the antenna.

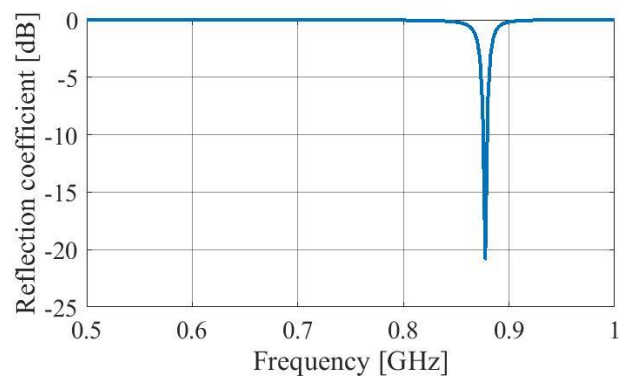


Figure 24: S-Parameter results of the ON state for FMIoT

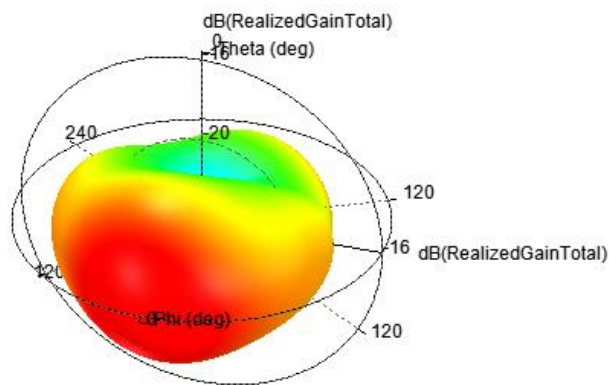


Figure 25: Realized gain of the ON state for FMIoT

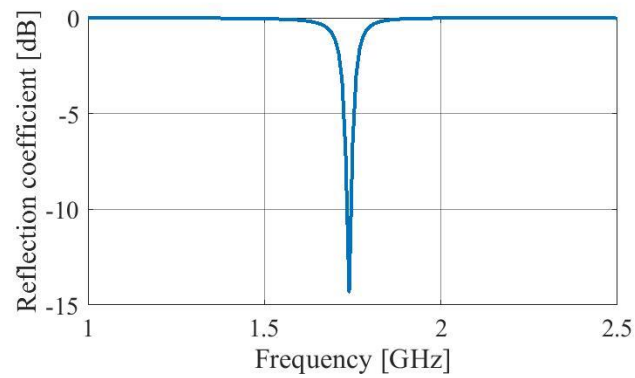


Figure 26: S-Parameter results of the OFF state for FMIoT

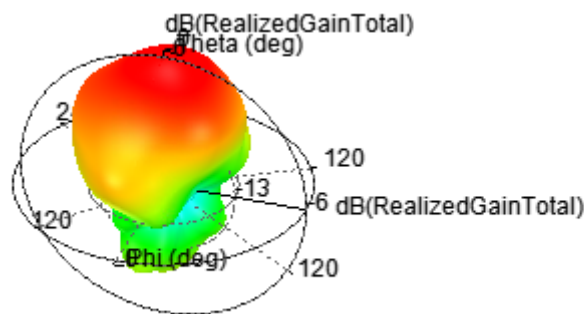


Figure 27: Realized gain for the OFF state for FMIoT

QGA is then reapplied on the antenna structure in the purpose of finding the best possible design. The code is not able to reach the frequency of 2.4 GHz as was our objective. As a result, the structure of our designed antenna is unable to reach that frequency. Our solution was to change in the physical structure of the antenna. The fitness function is shown in figure 28 where we can see that the fitness function increases with each iteration until reaching a maximum value after iteration 33.

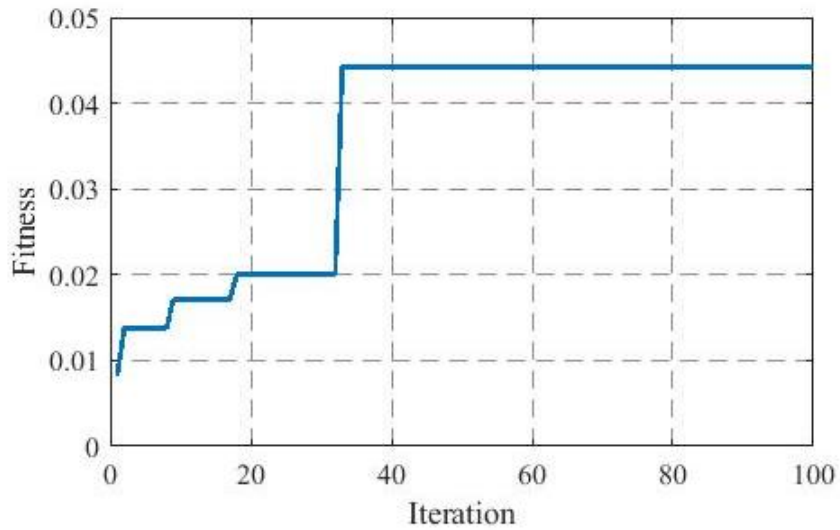


Figure 28: Fitness of the QGA

Table 4.1: Frequency values for the ON and OFF states of the pin diode

Optimization technique	GA		QGA	
PIN diode state	ON	OFF	ON	OFF
Frequencies (GHz)	0.8775	1.74	0.89	1.71
	0.8925	1.71	0.9	1.74

Table 4.1 shows the different frequencies of operation obtained after applying GA and QGA on the FMIoT for the ON and OFF states of the PIN diode. As we can see we are able to reach a frequency value around 0.868 GHz for the ON state of the pin diode, but a frequency around 2.4 GHz is not reachable with this current design. In addition, the gain on both ON and OFF states is negative.

As a result, since using pin diodes and vias can degrade the efficiency and gain of the antenna, our next step was to eliminate the vias, and replace the pin diode by an RF MEM in the following antenna designs because RF MEMS prove to have less effect on the antenna efficiency and gain.

3. Design three: new folded structure

We restarted with a new antenna design and we did it by the conventional way. First folding is applied to the antenna structure in order to minimize its physical size and by that achieve miniaturization.

As a first step, a patch antenna operating at 2.38 GHz is designed as shown in figure 29. The maximum realized gain of this patch is 4 dB as represented in figure 30. The patch, the ground plane and the substrate are folded as shown in figure 31. The operating frequency of the resulting antenna is 2.34 GHz with a realized gain of 3.21 dB as shown in figure 32. Folding the antenna, a second time as shown in figure 33, results in an antenna operating at 2.35 GHz with a realized gain of 2.64 dB as shown in figure 34. After several folding stages the final prototype shape is shown in figure 35. Folding the antenna decreases its physical size while maintaining the same frequency of operation [26].

The complete structure of the antenna forms a 3D folded patch topology with eight parts. In all parts of the antenna, three layers create its structure. The first layer is the radiating patch; the second layer is the Rogers Duroid Substrate 5880 with a dielectric constant of 2.2 and a thickness of 0.79 mm. The third layer is the ground plane that is covering the bottom layers of all sections. The final overall dimensions of the antenna are 40 mm x 52 mm x 5.16 mm. As shown in figure 36, this prototype operates at 2.36 GHz with a maximum realized gain of 2.21 dB.

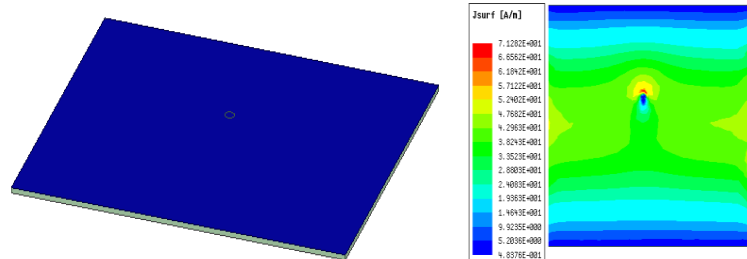


Figure 29: Antenna and its current's distribution

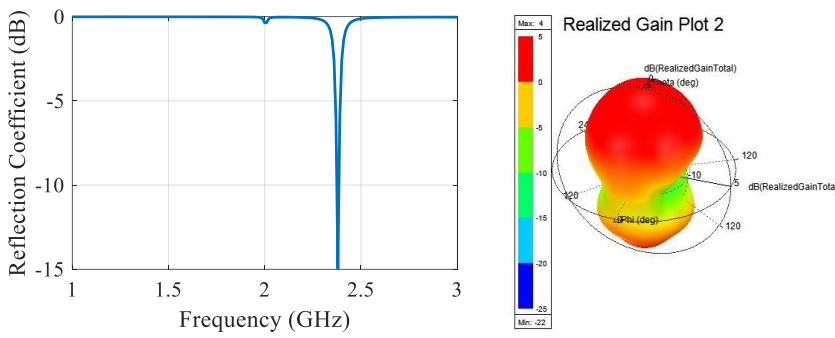


Figure 30: S-parameter and realized gain

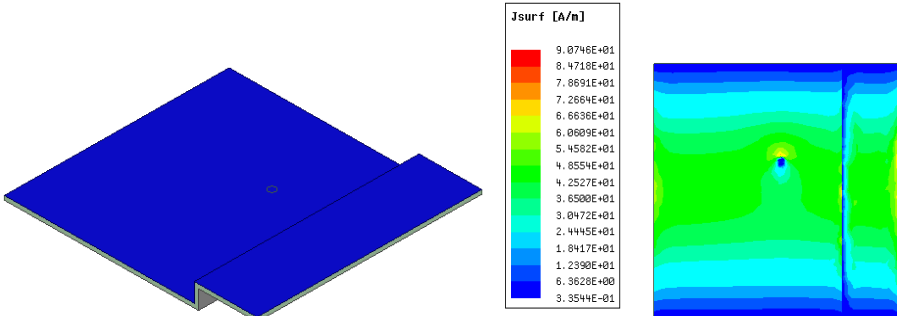


Figure 31: Antenna and Current distribution on the antenna's patch

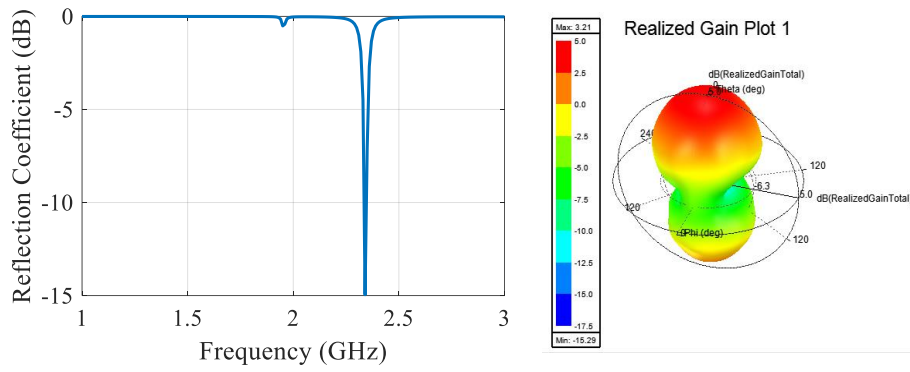


Figure 32: S-Parameter and realized gain

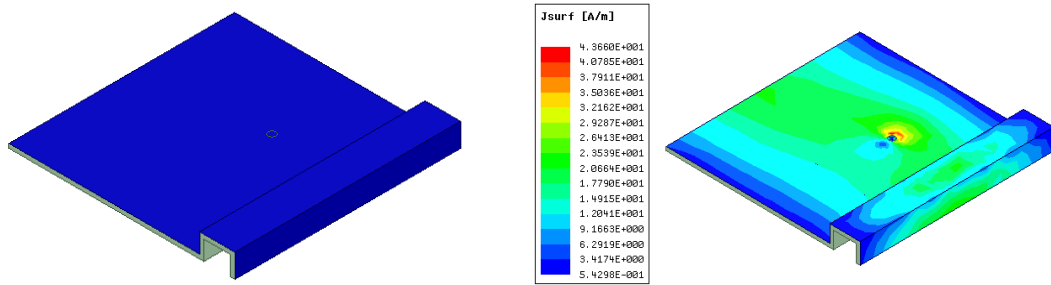


Figure 33: Antenna and Current distribution on the antenna's patch

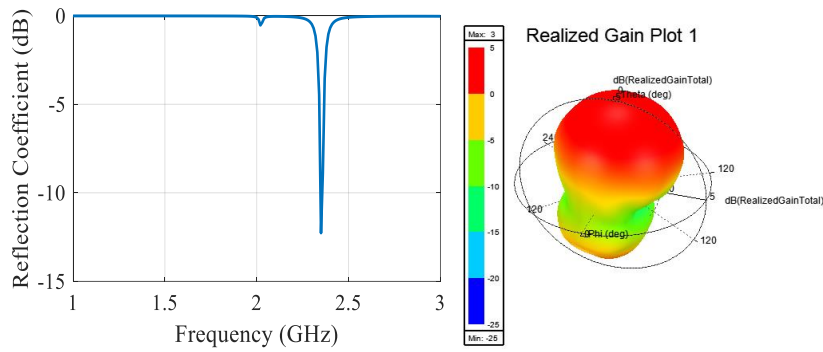


Figure 34: S-Parameter and Realized gain

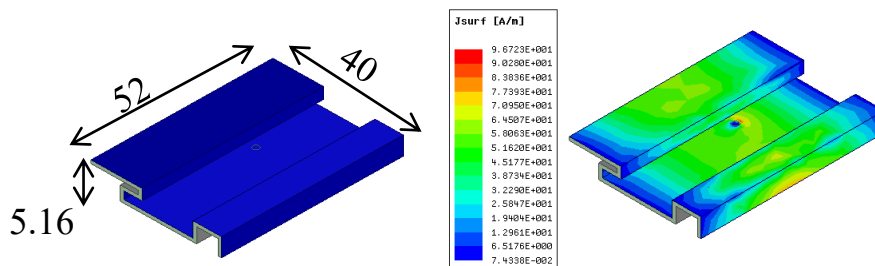


Figure 35: Antenna and Current distribution on the folded antenna's patch

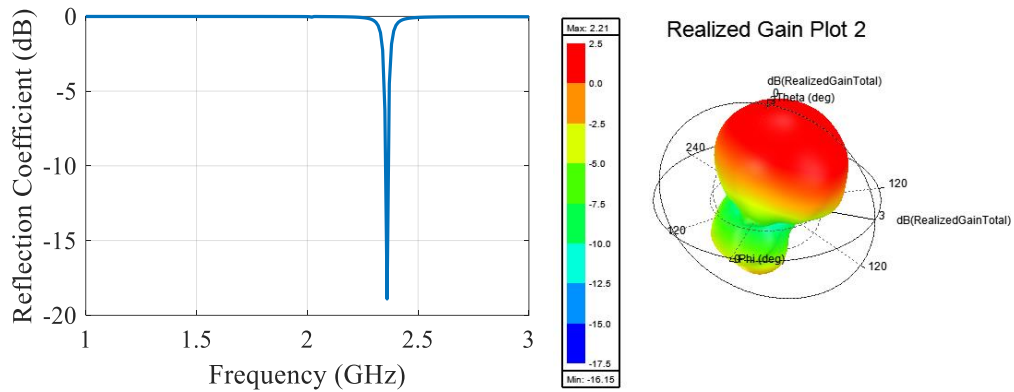


Figure 36: S-Parameter and realized gain of the folded antenna.

Our next step is to further miniaturize this folded antenna by adding slits and slots to the patch so that the antenna can operate at a frequency around 868 MHz. The design of the antenna in this case is achieved by solely relying on the electromagnetic principles, antenna theory and monitoring current distributions. In fact, the position of the slits and slots was determined relying on the current distribution on the patch. The position of the coax feed is optimized using parametric estimation in AED. The antenna is shown in figure 37. This antenna resonates at around 868 MHz with a maximum realized gain of -4 dB as shown in figure 38.

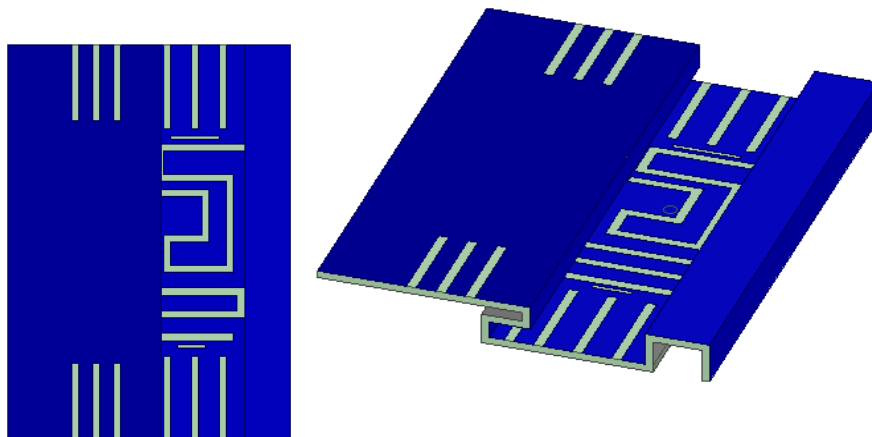


Figure 37: Simple antenna design

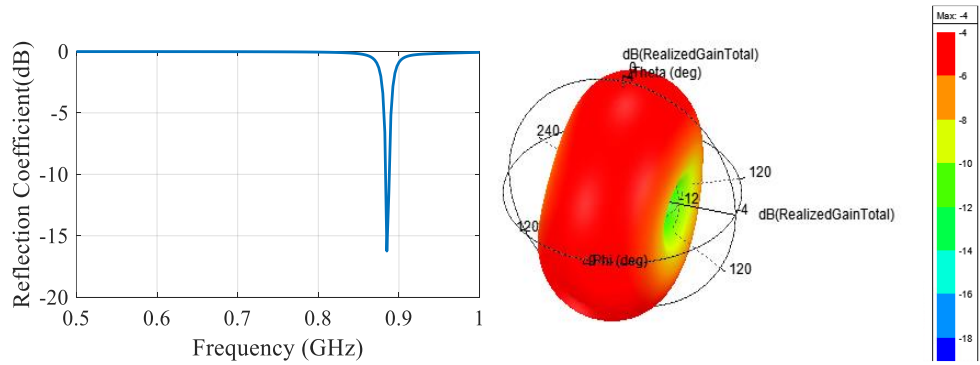


Figure 38: S-Parameter and realized gain of the simple antenna design

Our first objective was reached; we were able to design a miniaturized antenna that can be integrated in an IoT platform. The next objective was to make this antenna operating at 2.4 GHz in order to provide WIFI connectivity. So, the next step is to transform the obtained antenna to be reconfigurable. This time we are going to use RF MEMS in order to achieve this reconfiguration, since RF MEMS affect less the gain and the efficiency of the antenna. A parametric estimation for the best position of the RF MEMS was done. The resulting antenna design is shown in figure 39.

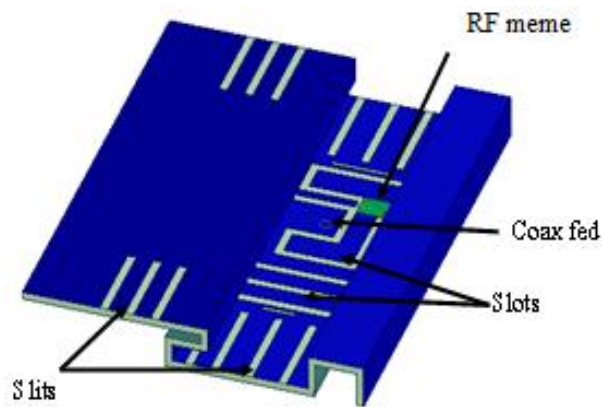


Figure 39: Simple reconfigurable antenna design

For the OFF state we can see a matching at around 868 MHz (fig. 40) with a gain of -4.14 dB (fig.41). In the ON state we can see a matching at 2.4 GHz (fig.42) with a gain of 2.47 dB (fig.43).

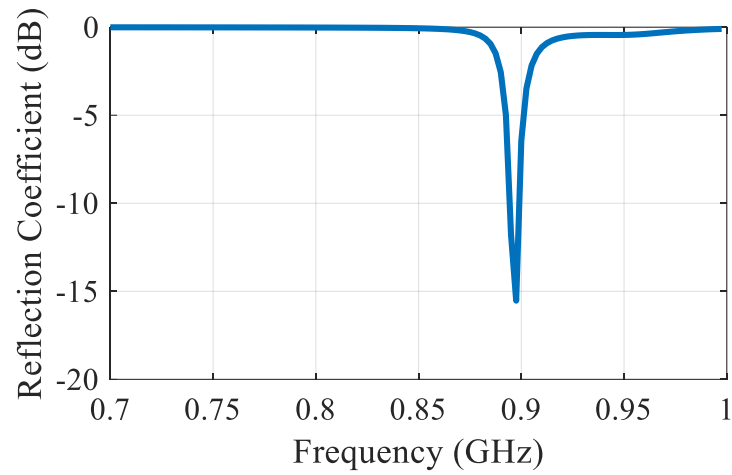


Figure 40: Reflection coefficient of the OFF state

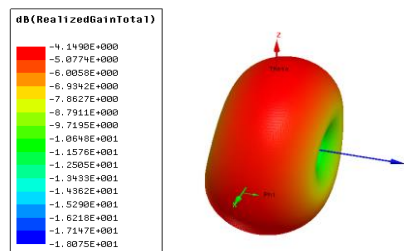


Figure 41: Realized gain on the OFF state

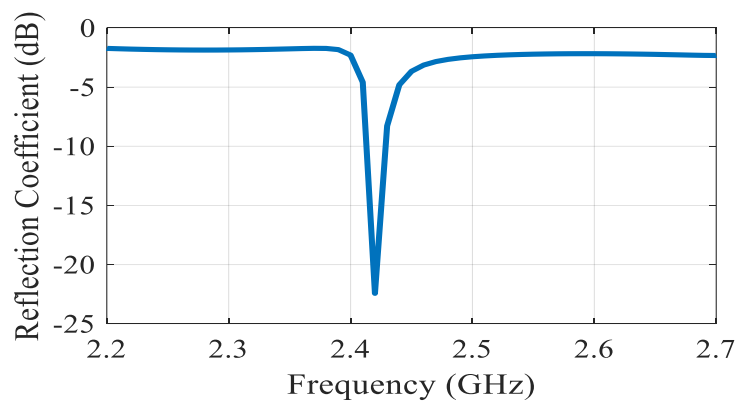


Figure 42: Reflection coefficient of the ON state

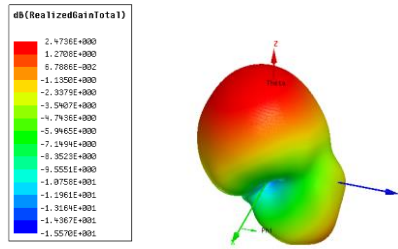


Figure 43: Realized gain of the ON state

As we can see the gain on the higher frequency improved and became positive in comparison with the previous design. In addition, we were able to reach a frequency around 2.4 GHz which was not the case for the previous design. But this design is not the best optimal design, because it does not give us the best optimal position of the slits and slots. So applying optimization algorithms is a must in order to reach the best optimal design.

4. Design 4: new folded QGA structure

After minimizing the physical size of the antenna, the next step is to reduce the operating frequency in order to reach 868 MHz. The presented antenna targets the IoT band. In order to reach the desired frequency of 868 MHz slots, slits must be added to the design. QGA is used to optimize the best positions of the pixilated slots in order to miniaturize the antenna and reach the frequency of 868 MHz. In fact, QGA introduces some views of quantum computing into GA. As seen before QGA accelerates the convergence process and progresses the parallelism of the genetic manipulation. [49].

QGA is used to reach the frequency 868 MHz and by that miniaturize the antenna by 87%. The obtained antenna is shown in figure 44, where the position of the pixilation is detailed.

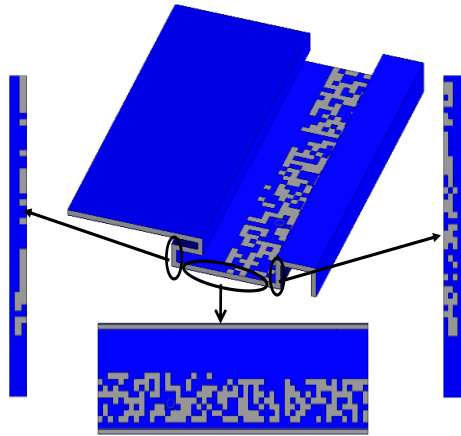


Figure 44: Antenna design using QGA

First, the code written to trigger the QGA starts with a population of 20 chromosomes; each chromosome represents a sequence of bits that will be mapped into an independent code for an independent antenna design. The total size of each chromosome is 1612 bits. The patch antenna is divided into 1612 cells. Each of these cells represents a conducting or non-conducting element. These binary bits represent the location of the pixelation on the antenna patch in addition to the location of the coax fed.

The first step of the code is the initialization of the Quantum chromosomes. The second step is the transformation of the quantum bits of each quantum chromosome into binary bits using a random pick.

The size of the lower layer of the patch is 16mm*52 mm as shown in figure 45. In the code we determine that 27% of the lower layer of the patch in the antenna must be slotted. So, we divide the first layer of the patch into 832 pads, each one of them having a size of 1 mm by 1 mm, an overlap of 0.1mm is added between the pads.

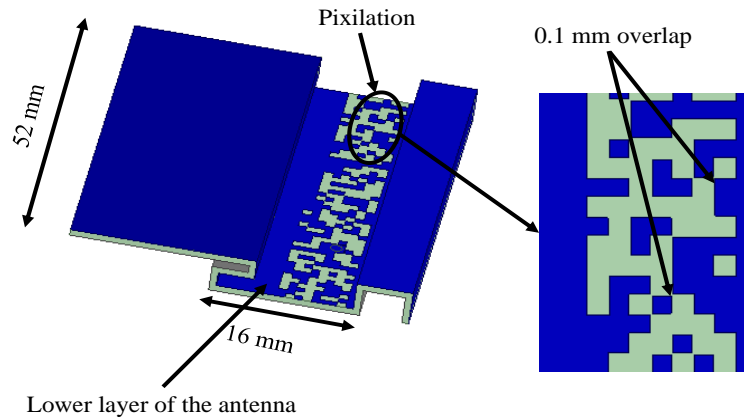


Figure 45: Pixilation in the lower layer of the antenna

The right and left vertical layers contain pixilated slots. The right vertical layer has dimensions of 3.58 mm x 52 mm as shown in figure 46. We divide this part into 293 pads where 20 % of them are slots. The dimensions of the slots in this layer are 0.5 mm in the z-direction and 1 mm in the x-direction. An overlap of 0.1 mm is applied to the pixilated slots.

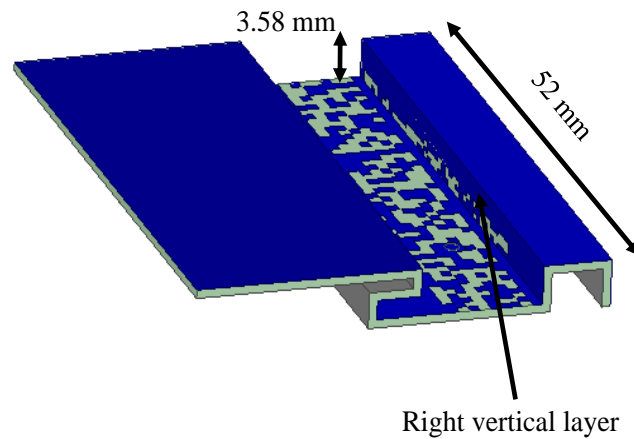


Figure 46: Pixilation in the right layer of the antenna

The left vertical layer has dimension of 1.79 mm x 52 mm as shown in figure 47. We divide this part into 125 pads where 24 % of them are slots. The dimensions of the slots in this layer are 0.5 mm in the z-direction and 1 mm in the x-direction. An overlap of 0.1 mm is applied to the pixilated slots.

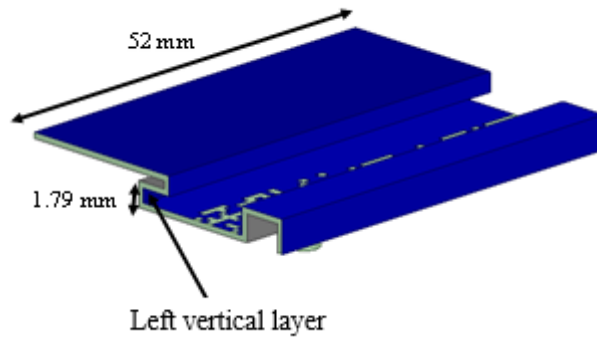
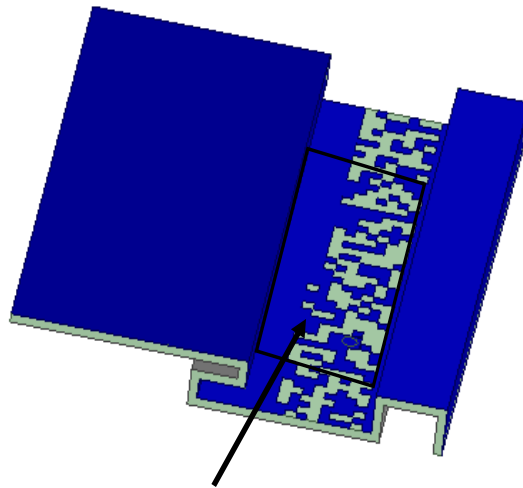


Figure 47: Pixilation in the left layer of the antenna

In addition, the position of the coax feed must be optimized by the code. 360 bits are specified in the chromosomes to determine the position of the coax. These 360 bits represent a window in the lower layer of the antenna where the coax feed can be present as shown in figure 48. In addition, the reflection coefficient and realized gain of the QGA antenna are shown in figure 49.

To represent these cells in the algorithm a binary coding is done with 1612 bits. 832 bits of the chromosomes are allocated to determine the position of the pixilation in the lower layer of the patch, 293 bits are allocated to determine the position of the pixilation in the right vertical layer, 125 bits are allocated to determine the position of the pixilation in the left vertical layer, and 360 bits are allocated to determine the position of the coax fed. The purpose of the code is to optimize the best positions of the different slots in the antenna.



Allocated zone where the coax fed can be

Figure 48: Possible zone of the coax fed

The code transforms the chromosomes into VBSCRIPT files, MATLAB runs these VBSCRIPT files in AED. The frequency having the lowest S11 is selected. The parameters used for training, which are the S-Parameters, the frequency and the gain, are extracted from AED. The fitness function plays a crucial role in optimization, this fitness is compiled by MATLAB. This fitness function must be designed in a way to find the optimized solution with the best efficiency, bandwidth and gain.

The fitness of each chromosome is calculated. The chromosome with the best fitness, and the fitness of this chromosome are saved. The quantum population is entered to a quantum gate. These quantum bits are transformed into binary bits. These steps are repeated for 100 iterations. The code is run on a windows 7 computer, which is characterized by a 64-bit operating system with a 32 GB installed memory (RAM). Its processor is Intel® Core™ i7-4770 CPU @3.40 GHz. The code is run for 100 iterations. The percentage of the fitness for each iteration is shown in figure 50. The maximum percentage reaches 97 % of the best possible fitness that we can reach. 100% of the fitness represent the best possible design that we can reach. As much as we approach from the 100% as must as we reach our best possible design.

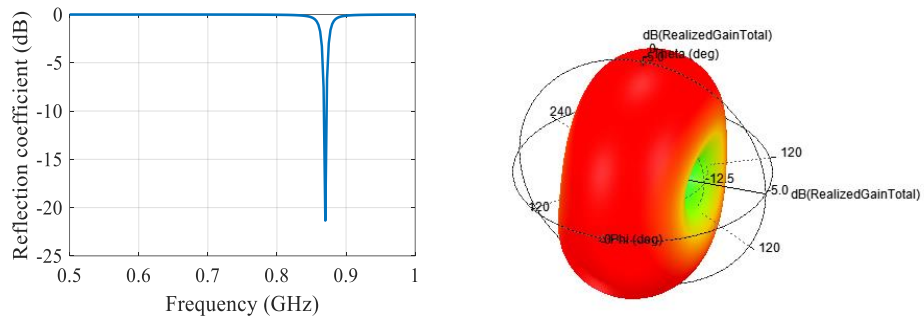


Figure 49: S-Parameter and realized gain of the QGA antenna

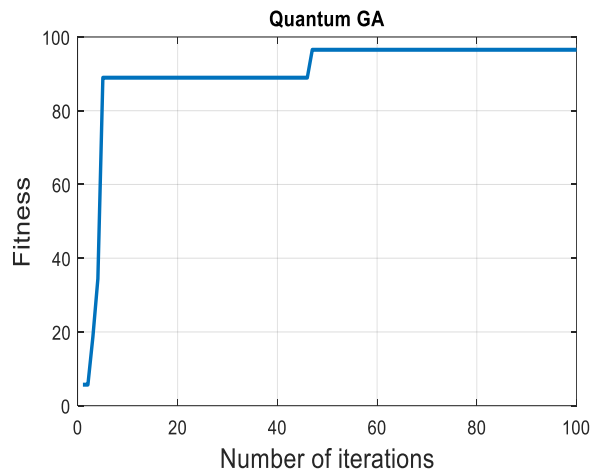


Figure 50: Percentage of the fitness with respect to the number of iterations

The antenna is fabricated using a mechanical milling machine. The fabrication is completed layer by layer, and then soldering is executed in order to assemble the different parts into the 3D final design. The fabricated design is shown in figure 51.

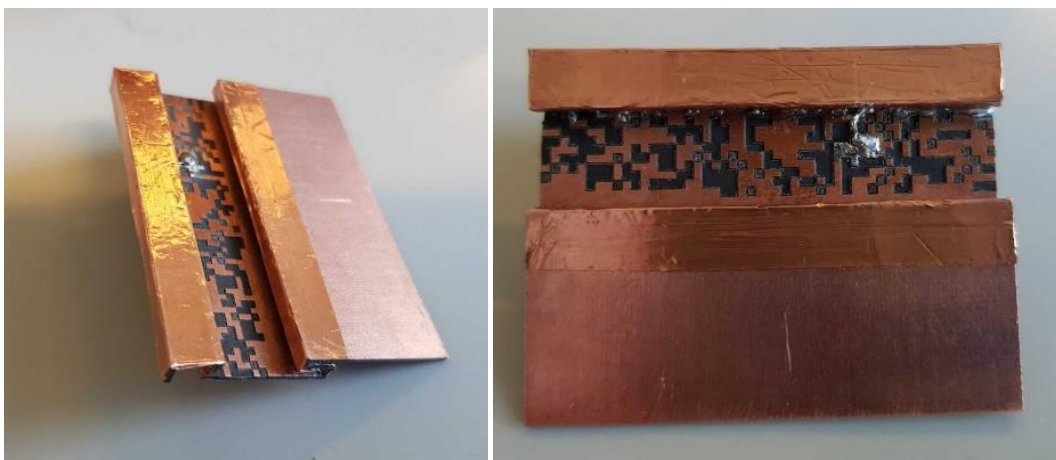


Figure 51: Fabricated prototype

5. Design 5: new folded reconfigurable QGA structure

After miniaturizing the antenna structure, frequency reconfiguration is sought in order to enable the antenna to operate at the frequencies 0.868 and 2.4 GHz for different configurations. A QGA code is employed in order to optimize the position of the slots in the three different layers of the antenna, the position of the coax feed, and the best position of the RF MEMS. 300 more bits are added to the different chromosomes of each population. These bits represent the possible positions of the RF MEMS. Each chromosome is now mapped to two different VBScripts, one of the VBS is for the ON state of the RF MEMS and the other is for the OFF state of the RF MEMS. After running these VBS files, and for each chromosome, we obtain a different S11, frequency and gain for the ON state and another set for the OFF state of the RF MEMS. These results are saved into an excel files and then they are imported to MATLAB where the fitness function (Eq.9) is calculated for each chromosome of the population. The new fitness function is the summation of two parts. One for the ON state and the other for the OFF state.

Cost=

$$\frac{(10 * (abs(frequencyON) - 0.868) + 1)}{((\exp(\frac{gainON}{4})) * abs(S11ON))} + \frac{(10 * (abs(frequencyOFF) - 2.4) + 1)}{((\exp(\frac{gainOFF}{4})) * abs(S11OFF))}$$

(Eq.9)

The obtained reconfigurable design is shown in figure 52.

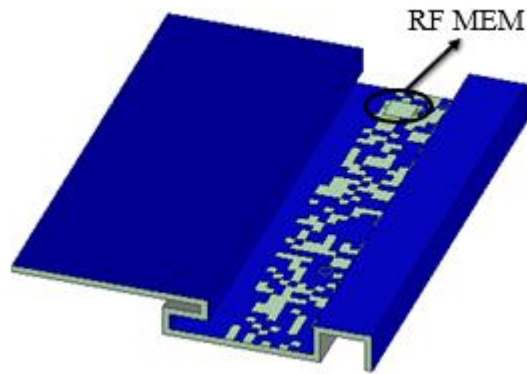


Figure 52: Reconfigurable QGA antenna design

The code is run for 10 days and the following results are obtained after 100 iterations where a 92 % of the best target fitness is reached, as shown in figure 53.

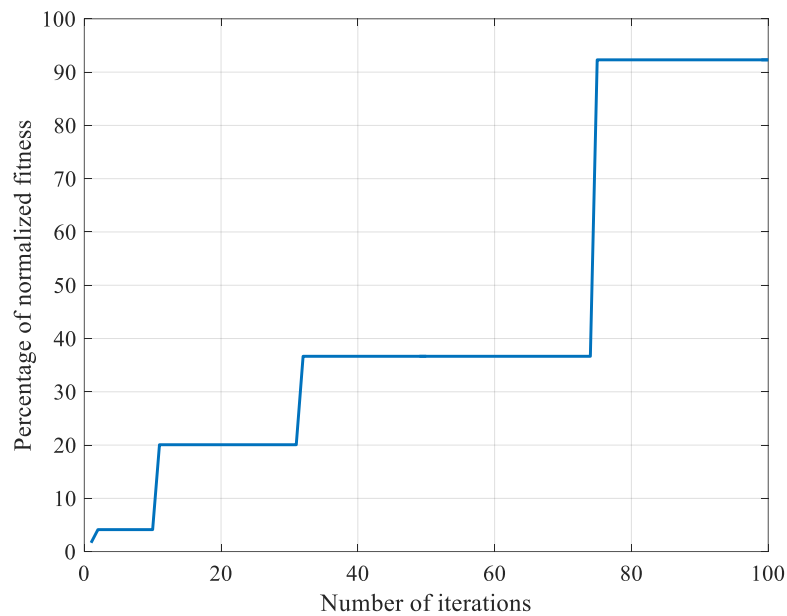


Figure 53: Percentage of the normalized fitness in function of the number of iterations

In the Off state we have a matching at 868 MHz (Fig.54) with a gain of -5.19 dB.(fig.55). In the On state we have matching at 2.4 GHz as shown in figure 56. With a gain of 2.14 dB in figure 57.

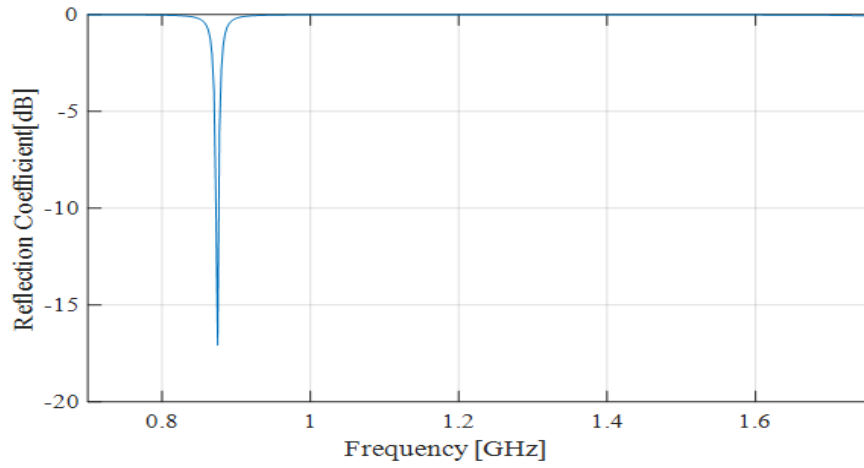


Figure 54: S parameter in the OFF state

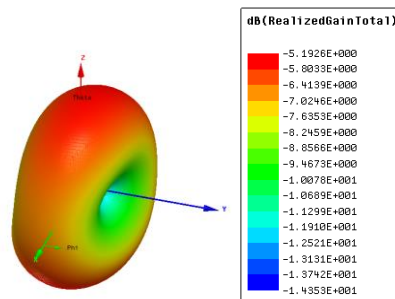


Figure 55: Realized gain in the OFF state

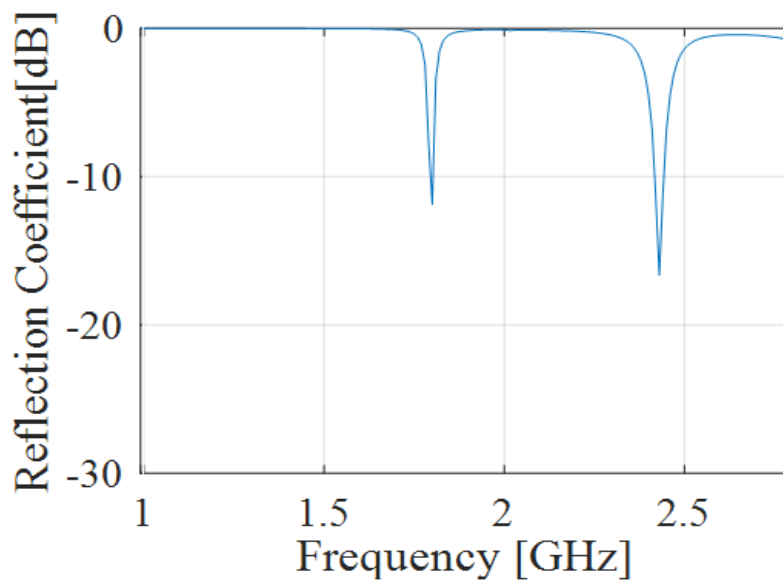


Figure 56: S-parameter of the ON state

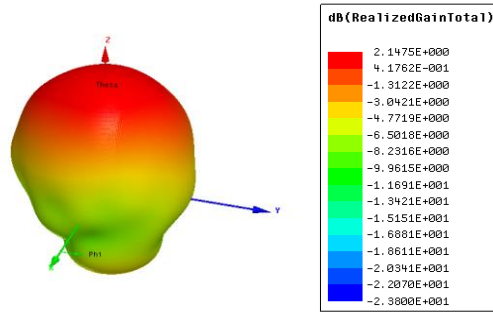


Figure 57: Realized gain of the ON state

F. Conclusion

Many objectives were targeted in our work. Our first objective was to design miniaturized antennas to be integrated in IoT platform. Different miniaturization techniques were used to achieve that including folding, slit and slots loading, shortening vias loading, in addition to using optimization algorithms. The miniaturized antennas target a frequency around 868 MHz. The second objective was to make these antennas reconfigurable in order to ensure Wifi connectivity. A frequency of 2.4 GHz was required. Two type of switches, pin diodes and RF MEMS, were used in our different designs to achieve miniaturization. Many techniques were used to find the best optimal position of the switch. GA and QGA algorithms were applied in some of the designs in order to reach the best optimal antennas configurations.

Table 4.2 summarizes the different reconfigurable antennas designed in this thesis with the techniques used, in addition to the simulated S11, and gain for the higher and lower frequencies of operation.

Table 1.2: Comparison between different reconfigurable antenna designs of the thesis

Reconfigurable Antenna	Optimization technique	Lower frequency (LF)	S11_LF	Gain_LF	Upper frequency (UF)	S11_UF	Gain_UF
FMIoT	GA	877	-21	-4.81	1.74	-14	-2.23
Simple folded	Traditional techniques	890	-16	-4.5	2.42	-24	2.47
FoMiP	QGA	868	-17	-5.19	2.4	-18	2.14

CHAPTER V

SMALL ANTENNA MEASUREMENTS

A. Introduction

Performance measurements of small antennas, whether reflection coefficient, or radiation efficiency are heavily affected by the measurement equipment as well as the environment. This is due to the miniature size of the radiating elements. In fact, small antennas are characterized by a low input resistance and a high input reactance. As a result, a traditional measurement of input impedance becomes not suitable. This chapter gives an overview of small antenna measurements; in addition, this chapter discusses the measurements done on the new designs proposed in this thesis.

B. Small Antenna measurements overview

One of the most common problems with the measurements of a small antenna is resides in the cables that are required to connect the antenna to a signal generator or a network analyzer. In fact the RF feed cables cause significant changes to the input impedance measured at the antenna port [61]. The movement of the antenna cable can alter the observed signal level significantly with variations of up to 10 dB. This problem can vary between antenna elements as well as it is frequency dependent [62-63].

An RF choke must always be used between the test cable and the antenna in order to suppress the cable currents [61]. It is also found that ferrite chokes on the exterior of the cables reduce the cable-related effect significantly.

A sleeve-like balun choke, shown in figure 58, when placed on the feed cable prevents surface currents of the Antenna Under Test (AUT) from passing to the outer shield of the RF feed cable [64]. Balun chokes are band limited but they are very effective in minimizing the effect of the leakage of the currents on the radiation of the antenna. The balun puts an “open end” termination at the edge of the AUT by enforcing a short circuit on the shield of the coaxial RF feed cable at a distance $\lambda/4$ from the edge of the AUT. The balun does not produce losses to the radiating platform. In addition, cascading multiple quarter-wave baluns can virtually cut the RF cable into small pieces, too short to act as radiating dipoles.

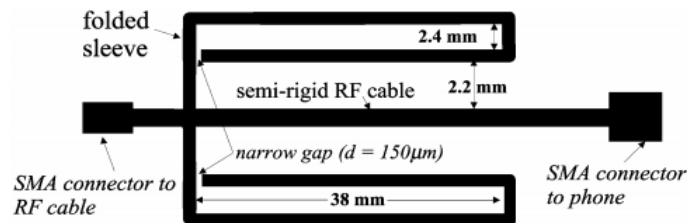


Figure 58: Cross section of the dual-band balun prototype [64]

Furthermore, placing lossy and absorbing material around the RF cable behind the balun can reduce the scattering effect to an acceptable level. Another alternative consists of incorporating Ferrite beads along with the balun in order to suppress the currents as shown in figure 59[64].



Figure 59: Ferrite beads and balun placed between the AUT and the cable for small antenna measurements [64]

In addition, small chambers (GTEM cells and small anechoic chambers) can be used for small antenna measurements. In fact, the gain, of a small antenna, measured in a GTEM cell has an average accuracy of ± 1 dB. Reciprocation is also achieved; the antenna under test can be a transmitter or a receiver without a change in the results.[65]

Some ways for small antenna measurements include the use of a contact-less measurement setup [66]. Rather than cable chokes, another option altogether is the implementation of an optics-based system to eliminate the possibility of cable currents. This system uses electro-optic transducers to enable delivery of the RF signal to the antenna under test using an optical fiber rather than a traditional coaxial cable [61].

Table 5.1 details the different measurement methods of small antennas along with their accuracy [66].

Table 2.1: Measurement methods for small antennas with their accuracy [55]

Measurement method	Accuracy (%)	Note
Pattern integration	<20	Suitable for most antennas. 3D radiation measurement required, time-consuming, and poor accuracy.
Direction/gain	<20	Suitable for a wide range of antennas, directional antennas.
Wheeler cap	<3	Suitable for electrically small antenna, cost effective, quick, accurate, and little data processing.

C. Measurements of the various proposed designs

Sliding wall cavity	<5	Suitable for many small antennas, cost effective. A special cavity required.
UWB Wheeler cap	<10	Suitable for Wideband and small antennas, cost effective, quick, and simple data processing.
Source-stirred cap/chamber	<5	Suitable for a wide range of antennas, cost effective, quick, and little data processing.
RC with a reference antenna	<10	Suitable for both large and small antennas and systems. A reference antenna with known radiation efficiency required, time consuming, and the frequency >LUF
RC without a reference antenna	<10	Suitable for both large and small antennas and no reference antenna required. A lengthy chamber calibration required and the frequency >LUF
Radiometric	<10	Suitable for many antennas. Special equipment required.
Q-factor	<10	Suitable for electrically small antennas, not as simple as the Wheeler cap method.
Calorimetric	<5	Suitable for small antennas and systems. A special heat flow comparator required

1. Design 1 FMIoT measurement

The FMIoT antenna satisfies the bandwidth upper limit constraint. It presents a 95 % size reduction with respect to a conventional patch antenna. The antenna's radiation efficiency is equal to 55.7% at the operating frequency. An overlap between the measured and simulated reflection coefficient is shown in figure 60, where good agreement is observed.

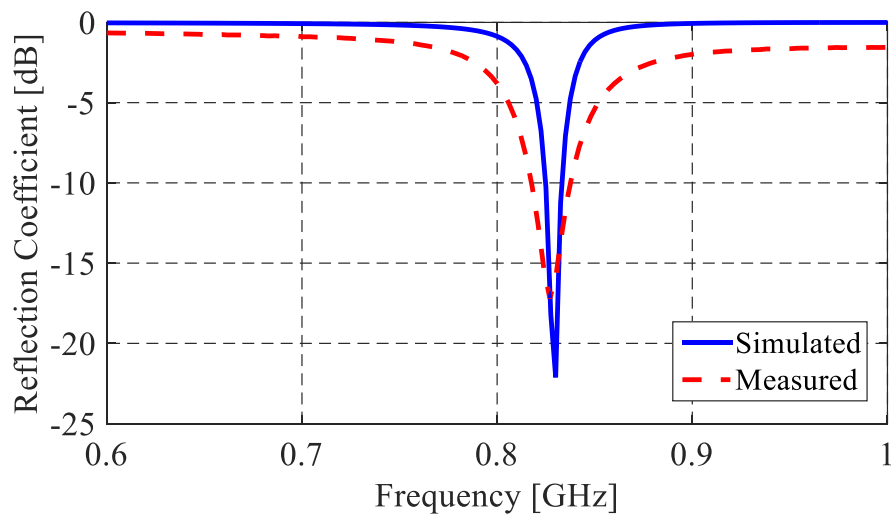


Figure 60: Simulated and measured reflection coefficient of FMIoT

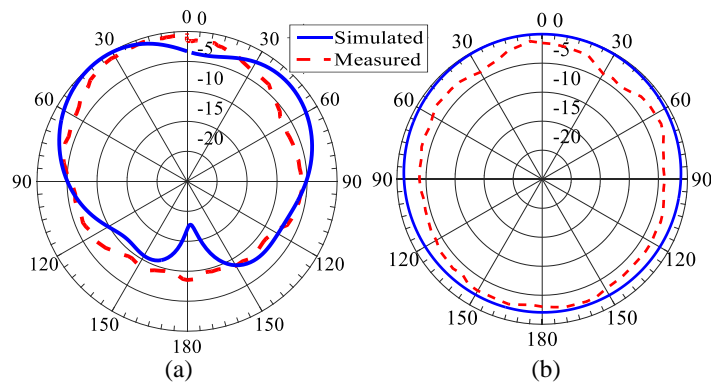


Figure 61: The radiation pattern of FMIoT at 820 MHz in the (a) X-Z plane and (b) X-Y plane.

Such antennas constitute the basis of IoT components, where size reduction and performance requirements are maintained and satisfied. Figure 60 shows that the FMIoT antenna operates at 820 MHz with a bandwidth of 30 MHz. In addition, the

radiation pattern of FMIoT at 820 MHz in the X-Z and X-Y planes are shown in figure 61.

In order to measure the reflection coefficient of the FMIoT antenna, a ferrite bead is placed on the cable and a balun is placed between the cable and the antenna as shown in figure 62. This is done in order to minimize the effect of the cable.



Figure 62: FMIoT antenna measurement using ferrite bead and a balun

Table 5.2 compares the FMIoT antenna with other antennas from literature, this antenna has a very high miniaturization with acceptable gain and efficiency.

Table 5.2: Characteristics of some miniaturized antennas

Dimension	Frequency	Bandwidth	Gain	Efficiency	Ref
0.082 λ_0 by 0.082 λ_0	820 MHz	30 MHz	-2.5 dB	65%	FMIoT
0.41 λ_0 by 0.41 λ_0 by 0.04 λ_0	3.5	58	2.7	63%	[67]
0.3 λ_0 by 0.26 λ_0 by 0.02 λ_0	From 2.5GHz to 11GHz	8.5 GHz	4 dBi		[68]

$0.8\lambda_g$ by $0.67\lambda_g$	2 GHz	190MHz	4.6 dBi	75%	[69]
$0.13 \lambda_0$ by $0.13 \lambda_0$	3 GHz	50 MHz	3.06	42%	[70]
$0.1\lambda_0$ by $0.1\lambda_0$ by $0.04\lambda_0$	1.227 GHz	580MHz	3 dB	54%,	[71]
$0.26 \lambda_0$ by $0.26 \lambda_0$ by $0.026 \lambda_0$.	(1.563–1.623 GHz)	60 MHz	0.91dBic	Not mentioned	[72]
$0.18\lambda_0$ by $0.18\lambda_0$ by $0.04\lambda_0$	2.38 GHz	35 MHz	-5.4 dBi	22%	[73]
$\pi 0.30 \lambda_0$ by 0.30 λ_0 by $0.045 \lambda_0$	4.42 GHz	227.5 MHz	1.1dB	Not mentioned	[74]
$0.173\lambda_0$ by $0.32\lambda_0$ by $0.0042\lambda_0$	0.8 GHz	≥ 20 MHz	-4 dB	Not mentioned	[75]
$0.125\lambda_0$ by $0.046\lambda_0$	433MHz 866 MHz		-5.3dBi - 0.7dBi	Not mentioned	[76]
$0.43 \lambda_0$ by $0.44 \lambda_0$	4.82 GHz	2.20	2.8 dB	93 percent	[77]
$0.12 \lambda_0$ by $0.12 \lambda_0$	2.42 GHz	Very narrow	-5 dB.	Not mentioned	[78]
$0.117 \lambda_0$ by 0.057 λ_0	880 MHz	30 MHz	-4.64 dBi	21%	[79]

2. Design 3 FoMiP measurement

The reflection coefficient in dB is measured using a vector network analyzer. To minimize the effect of the cable on the small antenna, a balun and ferrite beads are placed between the antenna and the cables (figure 63). An overlap of the simulated and measured reflection coefficient results is shown in figure 64 where good agreement is reached. The antenna is tested in the anechoic chamber. The radiation pattern of the antenna at 868 MHz in the X-Z plane and Y-Z plane are displayed in figure 65. An overlap of the simulated and fabricated results is done in Figure 65 where good agreement between the simulated and measurement results is obtained.



Figure 63: The prototype under measurement using a ballun and a ferrite bead

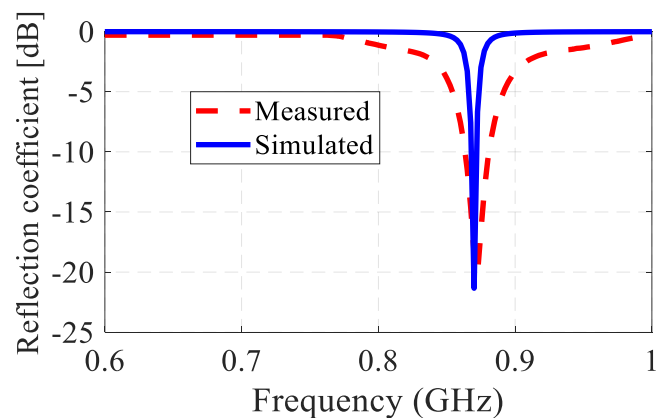


Figure 64: Simulation and measurement of S-Parameters

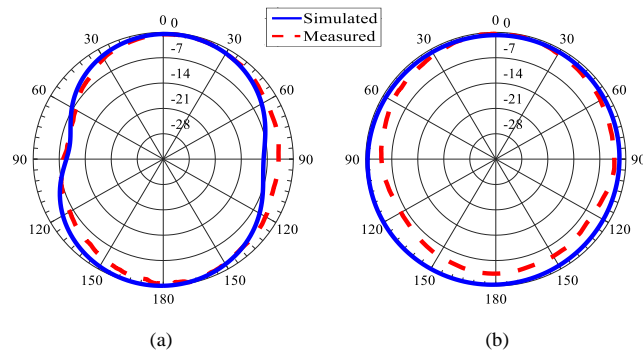


Figure 65: The radiation pattern of the antenna at 868 MHz in the (a) x-z plane and (b) y-z plane.

Table 5.3 compares the FoMiP antenna with different antennas in the literature.

The FoMiP antenna present good result in comparison with the other antennas.

Table 5.3: Characteristics of some miniaturized antennas

Dimension	Frequency	Bandwidth	Gain	Efficiency	Ref
0.11 λ_0 by 0.15 λ_0	858 MHz	30 MHz	-4.5 dB	75%	FOMiP
0.41 λ_0 by 0.41 λ_0 by 0.04 λ_0	3.5	58	2.7	63%	[67]
0.3 λ_0 by 0.26 λ_0 by 0.02 λ_0	From 2.5GHz to 11GHz	8.5 GHz (UWB)	4 dBi		[68]
0.8 λ_g by 0.67 λ_g	2 GHz	190MHz	4.6 dBi	75%	[69]
0.13 λ_0 by 0.13 λ_0	3 GHz	50 MHz	3.06	42%	[70]
0.1 λ_0 by 0.1 λ_0 by 0.04 λ_0	1.227 GHz	580MHz	3 dB	54%,	[71]
0.26 λ_0 by 0.26 λ_0 by 0.026 λ_0 .	(1.563–1.623 GHz)	60 MHz	0.91dBic	Not mentioned	[72]

0.18 λ_0 by 0.18 λ_0 by 0.04 λ_0	2.38 GHz	35 MHz	-5.4 dBi	22%	[73]
π 0.30 λ_0 by 0.30 λ_0 by 0.045 λ_0	4.42 GHz	227.5 MHz	1.1dB	Not mentioned	[74]
0.173 λ_0 by 0.32 λ_0 by 0.0042 λ_0	0.8 GHz	≥ 20 MHz	-4 dB	Not mentioned	[75]
0.125 λ_0 by 0.046 λ_0	433MHz- 866 MHz		-5.3dBi - 0.7dBi	Not mentioned	[76]
0.43 λ_0 by 0.44 λ_0	4.82 GHz	2.20	2.8 dB	93 percent	[77]
0.12 λ_0 by 0.12 λ_0	2.42 GHz	Very narrow	-5 dB.	Not mentioned	[78]
0.117 λ_0 by 0.057 λ_0	880 MHz	30 MHz	-4.64 dBi	21%	[79]

D. Conclusion

Conventional techniques cannot be used to measure small antennas. Reflection coefficient, radiation efficiency and other antenna parameters are deeply influenced by the measurement equipment as well as by the environment. This is due to the miniature size of the radiating elements. For example, RF feed cables cause significant changes to the input impedance measured at the antenna port. The movement of the antenna cable can alter the observed signal level significantly.

So an important parameter to account for when measuring small antennas is measurement small antenna techniques. This chapter introduced some techniques used for small antennas measurement. Two antennas which were developed in this thesis, the FMiOT and FoMiP, were measured using small measurement techniques. So, a balun was used between the small antenna under test and the RF cable, in addition ferrite bead was placed around the RF cable. This was done in order to minimize the effect of the cable.

CHAPTER VI

CONCLUSIONS AND FUTURE WORK

With the rise of the era of IoT, millions of devices are expected to interconnect on demand. Such pressing communication needs require dynamically reconfigurable miniaturized antennas to be present. The miniaturization aspect enables antennas to be integrated in compact IoT terminals, while the reconfiguration allows them to exhibit an agile communication scheme with diverse functionality.

Different techniques of miniaturization are presented in this thesis along a thorough analysis of their advantages and disadvantages. Some of the presented miniaturization techniques include folding, slits and slots loading, as well as shortening vias.

In addition, the designed antennas must be able to operate at 868 MHz to cater for IoT communication requirements and at the same must be able to connect to the internet on demand. Hence, another operational frequency of 2.4 GHz is needed. In order to achieve this reconfigurable operation, reconfiguration techniques are incorporated within antenna structures to redistribute their current for such agile behavior. Different reconfiguration mechanisms are investigated and analyzed, with the main focus residing on electrical switching tools. PIN diodes are replaced by RF MEMS in the proposed designs in order to preserve the radiation efficiency of the miniaturized elements.

The thesis also aims at wielding machine learning algorithms in order to result in optimal antenna designs. GA and QGA are utilized in order to optimize the antenna structure as well as the reconfiguration mechanism. Such optimization technique is completely automated through a novel code

that applies the various GA and QGA iterations onto the design space in AED. As a result, two different fitness functions are developed in this thesis. The first fitness is used for antenna miniaturization, and the other one focuses on adding reconfiguration into the miniaturized structures.

As a result, multiple antennas are proposed in this thesis. These antennas are miniaturized, reconfigurable and IoT suitable. The proposed antennas are measured by relying on small antenna measurement techniques and their realization is verified with predicted designs.

The work done in this thesis opens the door to implementing such antennas in more software controlled and aware environments such as in cognitive radio. Other future work involves including novel miniaturized antenna designs in a massive Multiple Input Multiple Output (MIMO) channels. Such channels and environments can mimic the IoT devices' communication schemes. Digital switches for reconfiguration are potential for integration into agile antennas. These digitally controlled switches enable a faster, swifter and more efficient reconfigurable control of the IoT communication systems. Optimization algorithms beyond GA and QGA can also be integrated into the design process of future miniaturized IoT antennas. In addition such algorithms can also optimize the connectivity of the billions of device within this futuristic communication environment.

REFERENCES

- [1] A. Holub and M. Polivka, "A Novel Microstrip Patch Antenna Miniaturization Technique: A Meanderly Folded Shorted-Patch Antenna," *2008 14th Conference on Microwave Techniques*, Prague, 2008, pp. 1-4.
doi: 10.1109/COMITE.2008.4569889
- [2] B. Ghosh, S. M. Haque and D. Mitra, "Miniaturization of Slot Antennas Using Slit and Strip Loading," in *IEEE Transactions on Antennas and Propagation*, vol. 59, no. 10, pp. 3922-3927, Oct. 2011.
doi: 10.1109/TAP.2011.2163754
- [3] C. Deng and Y. Xie, "Design of Resistive Loading Vivaldi Antenna," in *IEEE Antennas and Wireless Propagation Letters*, vol. 8, pp. 240-243, 2009.
doi: 10.1109/LAWP.2009.2013730
- [4] J. Jeon, K. Jang, S. Kahng and C. Park, "Design of a miniaturized UHF-band Zigbee antenna applicable to the M2M/IoT communication," *2014 IEEE Antennas and Propagation Society International Symposium (APSURSI)*, Memphis, TN, 2014, pp. 382-383.
doi: 10.1109/APS.2014.6904523
- [5] Y. Dong, J. Choi and T. Itoh, "Folded Strip/Slot Antenna With Extended Bandwidth for WLAN Application," in *IEEE Antennas and Wireless Propagation Letters*, vol. 16, pp. 673-676, 2017.
doi: 10.1109/LAWP.2016.2598276
- [6] N. Herscovici, M. F. Osorio and C. Peixeiro, "Miniaturization of rectangular microstrip patches using genetic algorithms," in *IEEE Antennas and Wireless*

Propagation Letters, vol. 1, pp. 94-97, 2002.

doi: 10.1109/LAWP.2002.805128

[7] N. Herscovici, M. F. Osorio and C. Peixeiro, "Minimization of a Rectangular Patch using Genetic Algorithms," *2005 18th International Conference on Applied Electromagnetics and Communications*, Dubrovnik, 2005, pp. 1-4.

doi: 10.1109/ICECOM.2005.204913

[8] C. Jarufe *et al.*, "Optimized Corrugated Tapered Slot Antenna for mm-Wave Applications," in *IEEE Transactions on Antennas and Propagation*, vol. 66, no. 3, pp. 1227-1235, March 2018.

doi: 10.1109/TAP.2018.2797534

[9] G. Chen, H. Jiang and X. Lei, "Reconfigurable antenna design optimization based on improved quantum genetic algorithm," *2014 XXXIth URSI General Assembly and Scientific Symposium (URSI GASS)*, Beijing, 2014, pp. 1-4.

doi: 10.1109/URSIGASS.2014.6929190

[10] Z. Abdullah, C. C. Tsimenidis and M. Johnston, "Quantum-inspired Tabu Search algorithm for antenna selection in massive MIMO systems," *2018 IEEE Wireless Communications and Networking Conference (WCNC)*, Barcelona, 2018, pp. 1-6.

doi: 10.1109/WCNC.2018.8377099

[11] Y. Tan, Y. Sun, Y. Zhu, D. Lauder and B. Ch, "Broadband impedance and antenna tuning using quantum genetic algorithms for multistandard wireless communications," *2015 Loughborough Antennas & Propagation Conference (LAPC)*, Loughborough, 2015, pp. 1-5.

doi: 10.1109/LAPC.2015.7366028

- [12] J. R. Perez and J. Basterrechea, "Genetic Algorithms for Predicting Antenna Radiation Patterns from Near-Field Measurements in a Screened Room," *2001 31st European Microwave Conference*, London, England, 2001, pp. 1-4.
doi: 10.1109/EUMA.2001.339018
- [13] J. Volakis, C. Chen, and K. Fujimoto, "Antennas: Miniaturization Techniques & Applications", 1st Edition.
- [14] R Steven, "A Study Of The Performance Properties Of Small Antennas" *The MITRE Corporation*, October 2007.
- [15] H. A. Wheeler, "Fundamental limitations of small antennas," *Proceedings of the IRE*, vol. 35, December 1947, pp. 1479-1484.
- [16] S. Pinhas and S. Shtrikman, "Comparison between computed and measured bandwidth of quarter-wave microstrip radiators," in *IEEE Transactions on Antennas and Propagation*, vol. 36, no. 11, pp. 1615-1616, Nov. 1988.
doi: 10.1109/8.9713
- [17] J. R. James, A. J. Schuler and R. F. Binham, "Reduction of antenna dimensions by dielectric loading," in *Electronics Letters*, vol. 10, no. 13, pp. 263-265, 27 June 1974.
doi: 10.1049/el:19740209
- [18] K. L. Wong and K. P. Yang, "Compact dual-frequency microstrip antenna with a pair of bent slots," in *Electronics Letters*, vol. 34, no. 3, pp. 225-226, 5 Feb. 1998.
doi: 10.1049/el:19980205
- [19] K. L. Wong and Y. F. Lin, "Small broadband rectangular microstrip antenna with chip-resistor loading," in *Electronics Letters*, vol. 33, no. 19, pp. 1593-1594, 11 Sept. 1997.
doi: 10.1049/el:19971111

- [20] T. K. Lo, Chun-On Ho, Y. Hwang, E. K. W. Lam and B. Lee, "Miniature aperture-coupled microstrip antenna of very high permittivity," in *Electronics Letters*, vol. 33, no. 1, pp. 9-10, 2 Jan. 1997.
doi: 10.1049/el:19970053.
- [21] S. Pinhas and S. Shtrikman, "Comparison between computed and measured band width of quarter-wave microstrip radiators," in *IEEE Transactions on Antennas and Propagation*, vol. 36, pp. 1615–1616, Nov. 1988.
- [22] R. B. Waterhouse, S. D. Targonski, and D. M. Kokotoff, "Design and performance of small printed antennas," in *IEEE Transactions on Antennas and Propagation*, vol. 46, pp. 1629–1633, Nov. 1998.
- [23] Y. J. Wang, C. K. Lee, W. J. Koh and Y. B. Gan, "Design of small and broad-band internal antennas for IMT-2000 mobile handsets," in *IEEE Transactions on Microwave Theory and Techniques*, vol. 49, no. 8, pp. 1398-1403, Aug. 2001.
doi: 10.1109/22.939919
- [24] H. Malekpoor and S. Jam, "Enhanced Bandwidth of Shorted Patch Antennas Using Folded-Patch Techniques," in *IEEE Antennas and Wireless Propagation Letters*, vol. 12, pp. 198-201, 2013.
doi: 10.1109/LAWP.2013.2244555
- [25] K.-L. Wong and K.-P. Yang, "Modified planar inverted-F antenna," *Electron. Lett.*, vol. 34, pp. 7–8, Jan. 1998
- [26] A. Holub and M. Polivka, "A Novel Microstrip Patch Antenna Miniaturization Technique: A Meanderly Folded Shorted-Patch Antenna," *2008 14th Conference on Microwave Techniques*, Prague, 2008, pp. 1-4.
doi: 10.1109/COMITE.2008.4569889

- [27] M. U. Khan, M. S. Sharawi, R. Mittra, "Microstrip patch antenna miniaturization techniques: a review" *IET Microwaves, Antennas & Propagation*, Dec. 2014, pp. 913-922
- [28] K. R. Jha, B. Bukhari, C. Singh, G. Mishra and S. K. Sharma, "Compact Planar Multi-Standard MIMO Antenna for IoT Applications," in *IEEE Transactions on Antennas and Propagation*.
doi: 10.1109/TAP.2018.2829533 (early access)
- [29] G. Oliveri *et al.*, "Design of compact printed antennas for 5G base stations," *2017 11th European Conference on Antennas and Propagation (EUCAP)*, Paris, 2017, pp. 3090-3093.
doi: 10.23919/EuCAP.2017.7928417
- [30] J. Costantine, Y. Tawk, S. E. Barbin and C. G. Christodoulou, "Reconfigurable Antennas: Design and Applications," in *Proceedings of the IEEE*, vol. 103, no. 3, pp. 424-437, March 2015.
doi: 10.1109/JPROC.2015.2396000
- [31] C. G. Christodoulou, Y. Tawk, S. A. Lane, and S. R. Erwin, "Reconfigurable Antennas for Wireless and Space Applications," *Proceedings of the IEEE*, 100(7), pp. 2250–2261, 2012. DOI:10.1109/JPROC.2012.2188249. 1,2,3,8
- [32] J. Costantine; Y. Tawk; C. Christodoulou, "Design of Reconfigurable Antennas Using Graph Models," in *Design of Reconfigurable Antennas Using Graph Models*, Morgan & Claypool, 2013
- [33] Y.Tawk, J.Costantine, and C.G.Christodoulou, "A frequency reconfigurable printed monopole with pattern diversity," *IEEE Trans. Antennas Propag.*, 2015.

- [34] Y. Tawk, J. Costantine and C. G. Christodoulou, "A Varactor-Based Reconfigurable Filtenna," in *IEEE Antennas and Wireless Propagation Letters*, vol. 11, pp. 716-719, 2012.
doi: 10.1109/LAWP.2012.2204850
- [35] C.W.Jung,M.Lee,G.P.Li,and F.DeFlaviis,“Reconfigurable scan-beam single-arm spiral antenna integrated with RF-MEMS switches,” *IEEE Transactions on Antennas and Propagation*,vol.54,no.2,pp.455–463,Feb.2006.DOI:10.1109/TAP.2005.863407.
1,4
- [36] Y. Tawk, J. Costantine and C. G. Christodoulou, "A reconfigurable band-reject MIMO for cognitive radio," *2013 7th European Conference on Antennas and Propagation (EuCAP)*, Gothenburg, 2013, pp. 1996-1998.
- [37] K.H. Han and J. H. Kim, "Quantum-inspired evolutionary algorithm for a class of combinatorial optimization," in *IEEE Transactions on Evolutionary Computation*, vol. 6, no. 6, pp. 580-593, Dec. 2002.
doi: 10.1109/TEVC.2002.804320
- [38] D. E. Goldberg, *Genetic algorithms in search, optimization, and machine learning.* Reading, MA: Addison-Wesley, 1989.
- [39] Kyohei Fujimoto, Hisashi Morishita, “Modern small antennas”, Cambridge University Press, 2013
- [40] T. D. Nguyen, T. P. Vuong, Y. Duroc and V. Y. Vu, "Optimization Of PIFA antenna using an auto-embedded Genetic Algorithm," *International Conference on Communications and Electronics 2010*, Nha Trang, 2010, pp. 367-372.
doi: 10.1109/ICCE.2010.5670652

- [41] J. W. Jayasinghe, J. Anguera, and D. N. Uduwawala, "A simple design of multi band microstrip patch antennas robust to fabrication tolerances for GSM, UMTS, LTE, and Bluetooth applications by using genetic algorithm optimization," *Progress In Electromagnetics Research M*, Vol. 27, 255–269, 2012
- [42] F. J. Villegas, T. Cwik, Y. Rahmat-Samii and M. Manteghi, "A parallel electromagnetic genetic-algorithm optimization (EGO) application for patch antenna design," in *IEEE Transactions on Antennas and Propagation*, vol. 52, no. 9, pp. 2424-2435, Sept. 2004.
doi: 10.1109/TAP.2004.834071
- [43] N. Jin and Y. Rahmat-Samii, "Hybrid Real-Binary Particle Swarm Optimization (HPSO) in Engineering Electromagnetics," in *IEEE Transactions on Antennas and Propagation*, vol. 58, no. 12, pp. 3786-3794, Dec. 2010.
doi: 10.1109/TAP.2010.2078477
- [44] N. Herscovici, M. F. Osorio and C. Peixeiro, "Miniaturization of rectangular microstrip patches using genetic algorithms," in *IEEE Antennas and Wireless Propagation Letters*, vol. 1, pp. 94-97, 2002.
doi: 10.1109/LAWP.2002.805128
- [45] K. Fertas, H. Kimouche, M. Challal, H. Aksas and R. Aksas, "An optimized shaped antenna for multiband applications using Genetic Algorithm," *2015 4th International Conference on Electrical Engineering (ICEE)*, Boumerdes, 2015, pp. 1-4.
doi: 10.1109/INTEE.2015.7416757
- [46] S. Sun, Y. Lv, J. Zhang, Z. Zhao and F. Ruan, "Optimization based on genetic algorithm and HFSS and its application to the semiautomatic design of antenna," *2010 International Conference on Microwave and Millimeter Wave Technology*, Chengdu,

2010, pp. 892-894.

doi: 10.1109/ICMMT.2010.5525163

[47] P. Soontornpipit, C. M. Furse and You Chung Chung, "Miniaturized biocompatible microstrip antenna using genetic algorithm," in *IEEE Transactions on Antennas and Propagation*, vol. 53, no. 6, pp. 1939-1945, June 2005.

doi: 10.1109/TAP.2005.848461

[48] S. K. Josan, J. S. Sohal and B. S. Dhaliwal, "Design of elliptical microstrip patch antenna using Genetic Algorithms," *2012 IEEE International Conference on Communication Systems (ICCS)*, Singapore, 2012, pp. 140-143.

doi: 10.1109/ICCS.2012.6406125

[49] G. Chen, H. Jiang and X. Lei, "Reconfigurable antenna design optimization based on improved quantum genetic algorithm," *2014 XXXIth URSI General Assembly and Scientific Symposium (URSI GASS)*, Beijing, 2014, pp. 1-4.

doi: 10.1109/URSIGASS.2014.6929190

[50] L. Li, G. Cui, X. Lv, X. Sun and H. Wang, "An Improved Quantum Rotation Gate in Genetic Algorithm for Job Shop Scheduling Problem," *2018 International Conference on Information Systems and Computer Aided Education (ICISCAE)*, Changchun, China, 2018, pp. 322-325.

doi: 10.1109/ICISCAE.2018.8666865

[51] K. Han and J. Kim, "Quantum-inspired evolutionary algorithm for a class of combinatorial optimization," in *IEEE Transactions on Evolutionary Computation*, vol. 6, no. 6, pp. 580-593, Dec. 2002.

doi: 10.1109/TEVC.2002.804320

- [52] Z. Abd El MoizDahi, C. Mezioud, and A. Draa, "A quantum-inspired genetic algorithm for solving the antenna positioning problem," *Swarm and Evolutionary Computation, Elsevier*, Dec. 2016
- [53] L. Shuguang and B. Lin, "Progress, Application and Prospect of Quantum Genetic Algorithm," *2018 IEEE International Conference on Electronics and Communication Engineering (ICECE)*, Xi'an, China, 2018, pp. 65-70.
doi: 10.1109/ICECOME.2018.8644838
- [54] G. Zhang, L.Hu, and W. Jin, "Resemblance coefficient and a quantum genetic algorithm for feature selection," *Lecture Notes Comput. Sci.*, vol. 3245, pp. 155–168, Jan. 2004.
- [55] M. Martinez, L. Longpre, V. Kreinovich, S. A. Starks and H. T. Nguyen, "Fast quantum algorithms for handling probabilistic, interval, and fuzzy uncertainty," *22nd International Conference of the North American Fuzzy Information Processing Society, NAFIPS 2003*, Chicago, IL, 2003, pp. 395-400.
doi: 10.1109/NAFIPS.2003.1226817
- [56] MATLAB - MathWorks", *Mathworks.com*, 2019. [Online]. Available: <https://www.mathworks.com/products/matlab.html>. [Accessed: 01- May- 2019].
- [57] "Electromagnetic Analysis | ANSYS Electronics Desktop", *Ansys.com*, 2019. [Online]. Available: <https://www.ansys.com/products/electronics/ansys-electronics-desktop>. [Accessed: 01- May- 2019].
- [58] VBScript Tutorial", *www.tutorialspoint.com*, 2019. [Online]. Available: <https://www.tutorialspoint.com/vbscript/>. [Accessed: 01- May- 2019].

- [59] *Ece.uprm.edu*, 2019. [Online]. Available:
<http://www.ece.uprm.edu/~rafaelr/inel6068/HFSS/scripting.pdf>. [Accessed: 01- May-2019].
- [60] R. M. Bichara, F. A. Asadallah, J. Costantine and M. Awad, "A Folded Miniaturized Antenna for IoT Devices," *2018 IEEE Conference on Antenna Measurements & Applications (CAMA)*, Vasteras, 2018, pp. 1-3.
doi: 10.1109/CAMA.2018.8530468
- [61] J. T. Bernhard, J. J. Adams, M. D. Anderson and J. M. Martin, "Measuring electrically small antennas: Details and implications," *2009 IEEE International Workshop on Antenna Technology*, Santa Monica, CA, 2009, pp. 1-4.
doi: 10.1109/IWAT.2009.4906959
- [62] C. Icheln, J. Ollikainen and P. Vainikainen, "Reducing the influence of feed cables on small antenna measurements," in *Electronics Letters*, vol. 35, no. 15, pp. 1212-1214, 22 July 1999.
doi: 10.1049/el:19990851
- [63] T. Fukasawa, K. Nishimoto, T. Yanagi and H. Miyashita, "Measurement methods for a small antenna with reduced influence of a measurement cable," *2014 IEEE International Workshop on Electromagnetics (iWEM)*, Sapporo, 2014, pp. 253-254.
doi: 10.1109/iWEM.2014.6963731
- [64] C. Icheln, J. Krogerus and P. Vainikainen, "Use of balun chokes in small-antenna radiation measurements," in *IEEE Transactions on Instrumentation and Measurement*, vol. 53, no. 2, pp. 498-506, April 2004.
doi: 10.1109/TIM.2004.823299

- [65] E. L. Bronaugh and J. D. M. Osburn, "Measuring antenna parameters in a GHz transverse electromagnetic (GTEM) cell," *IEEE Antennas and Propagation Society International Symposium 1992 Digest*, Chicago, IL, USA, 1992, pp. 2064-2066 vol.4.
doi: 10.1109/APS.1992.221461
- [66] Y. Huang (2015) Radiation Efficiency Measurements of Small Antennas. In: Chen Z. (eds) *Handbook of Antenna Technologies*. Springer, Singapore.
- [67] A. Boukarkar, X. Q. Lin, Y. Jiang, L. Y. Nie, P. Mei and Y. Q. Yu, "A Miniaturized Extremely Close-Spaced Four-Element Dual-Band MIMO Antenna System With Polarization and Pattern Diversity," in *IEEE Antennas and Wireless Propagation Letters*, vol. 17, no. 1, pp. 134-137, Jan. 2018.
doi: 10.1109/LAWP.2017.2777839
- [68] D. Yang, S. Liu and D. Geng, "A Miniaturized Ultra-Wideband Vivaldi Antenna With Low Cross Polarization," in *IEEE Access*, vol. 5, pp. 23352-23357, 2017.
doi: 10.1109/ACCESS.2017.2766184
- [69] S. S. Jehangir, M. S. Sharawi and A. Shamim, "Highly miniaturised semi-loop meandered dual-band MIMO antenna system," in *IET Microwaves, Antennas & Propagation*, vol. 12, no. 6, pp. 864-871, 23 5 2018.
doi: 10.1049/iet-map.2017.0701
- [70] A. Boukarkar, X. Q. Lin, Y. Jiang and Y. Q. Yu, "Miniaturized Single-Feed Multiband Patch Antennas," in *IEEE Transactions on Antennas and Propagation*, vol. 65, no. 2, pp. 850-854, Feb. 2017.
doi: 10.1109/TAP.2016.2632620
- [71] M. Wang, X. Zhu, Y. Guo and W. Wu, "Miniaturized Dual-Band Circularly Polarized Quadruple Inverted-F Antenna for GPS Applications," in *IEEE Antennas and*

Wireless Propagation Letters, vol. 17, no. 6, pp. 1109-1113, June 2018.

doi: 10.1109/LAWP.2018.2834484

[72] M. Wang, X. Zhu, Y. Guo and W. Wu, "Compact dual-band circularly polarised antenna with omnidirectional and unidirectional properties," in *IET Microwaves, Antennas & Propagation*, vol. 12, no. 2, pp. 259-264, 7 2 2018.

doi: 10.1049/iet-map.2017.0658

[73] X. Zhu, Y. Guo and W. Wu, "Miniaturized Dual-Band and Dual-Polarized Antenna for MBAN Applications," in *IEEE Transactions on Antennas and Propagation*, vol. 64, no. 7, pp. 2805-2814, July 2016.

doi: 10.1109/TAP.2016.2556701

[74] W. Cao, "Compact dual-band dual-mode circular patch antenna with broadband unidirectional linearly polarised and omnidirectional circularly polarised characteristics," in *IET Microwaves, Antennas & Propagation*, vol. 10, no. 2, pp. 223-229, 29 1, 2016.

doi: 10.1049/iet-map.2015.0266

[75] K. R. Jha, B. Bukhari, C. Singh, G. Mishra and S. K. Sharma, "Compact Planar Multi-Standard MIMO Antenna for IoT Applications," in *IEEE Transactions on Antennas and Propagation*.

doi: 10.1109/TAP.2018.2829533 (early access)

[76] A. Selek, C. Turkmen and M. Secmen, "Compact planar folded monopole antenna with coupling mechanism for Quad ISM band, GNSS and UMTS applications," *2018 11th German Microwave Conference (GeMiC)*, Freiburg, 2018, pp. 211-214.

doi: 10.23919/GEMIC.2018.8335067

[77] S. Koziel and A. Bekasiewicz, "Design optimization of novel compact circular polarization antenna," *2018 International Applied Computational Electromagnetics Society Symposium (ACES)*, Denver, CO, 2018, pp. 1-2.

doi: 10.23919/ROPACES.2018.8364093

[78] M. A. Abdalla and S. Safavi-Naeini, "A new configuration for ultra compact implantable antenna based on SIW L-CRLH concept," *2017 IEEE International Symposium on Antennas and Propagation & USNC/URSI National Radio Science Meeting*, San Diego, CA, 2017, pp. 541-542.

doi: 10.1109/APUSNCURSINRSM.2017.8072313

[79] G. Oliveri *et al.*, "Design of compact printed antennas for 5G base stations," *2017 11th European Conference on Antennas and Propagation (EuCAP)*, Paris, 2017, pp. 3090-3093.

doi: 10.23919/EuCAP.2017.7928417